



Published in final edited form as:

Mol Neurobiol. 2018 August ; 55(8): 6713–6733. doi:10.1007/s12035-018-0878-2.

Morphine-mediated brain region-specific astrocytosis involves the ER stress-autophagy axis

Susmita Sil¹, Palsamy Periyasamy¹, Ming-Lei Guo¹, Shannon Callen¹, and Shilpa Buch¹

¹Department of Pharmacology and Experimental Neuroscience, University of Nebraska Medical Center, Omaha, NE 68198-5880, USA.

Abstract

A recent study from our lab has revealed a link between morphine-mediated autophagy and synaptic impairment. The current study was aimed at investigating whether morphine-mediated activation of astrocytes involved the ER stress/autophagy axis. Our *in vitro* findings demonstrated upregulation of GFAP indicating astrocyte activation with concomitantly increased production of proinflammatory cytokines in morphine-exposed human astrocytes. Using both pharmacological and gene-silencing approaches, it was demonstrated that morphine-mediated defective autophagy involved upstream activation of ER stress with subsequent downstream astrocyte activation via the μ -opioid receptor (MOR). Validation *in vivo* demonstrated preferential activation of ER stress/autophagy axis in the areas of the brain not associated with pain such as the basal ganglia, frontal cortex, occipital cortex and the cerebellum of morphine-dependent rhesus macaques, and this correlated with increased astrocyte activation and neuroinflammation. Interventions aimed at blocking either the MOR or ER stress could thus likely be developed as promising therapeutic targets for abrogating morphine-mediated astrocytosis.

Keywords

astrocytosis; defective autophagy; ER stress; morphine; neuroinflammation; rhesus macaques

Introduction

Morphine is the most potent painkiller among all the opiates and is used extensively in the clinical settings [1], because of its comfort giving properties including drowsiness, relief from anxiety, and euphoria [2]. With the increased morbidity associated with pain-related conditions such as cancer, morphine abuse has escalated worldwide and has become a serious global problem [3]. It has been reported that almost half of the accidental drug deaths can be attributable to morphine or heroin overdose [4]. Chronic exposure to morphine leads to increased complications such as addiction, tolerance, cognitive impairment, withdrawal, and severely compromised immune system with an increased risk of

CONTACT: Dr. Shilpa Buch, Department of Pharmacology and Experimental Neuroscience, University of Nebraska Medical Center, Omaha, NE 68198-5880, USA. sbuch@unmc.edu.

Conflict of Interest

The authors declare no competing financial interests.

among ER stress, autophagy and neurodegenerative disorders such as Alzheimer disease, Parkinson disease, and prion disease [47,48]. Essentially, ER stress is regulated by three ER membrane-embedded sensor proteins: inositol-requiring protein 1 α (IRE1 α), protein kinase R-like ER kinase (PERK), and activating transcription factor 6 (ATF6) that restore the ER homeostasis. Several studies have also implicated the regulatory role of PERK in ER stress-mediated autophagy [49,46]. Drugs of abuse such as cocaine under various experimental conditions have been shown to mediate ER stress, which in turn, regulates the expression of different genes involved in microglial and astrocyte autophagy [50,37]. Morphine-mediated autophagy has also been reported in various cell types, such as bone marrow-derived macrophages [51], neuroblastoma cell line [52], primary hippocampal neurons [43], and microglia [53]. The specific role of morphine in the activation of astrocytes, possibly through ER stress-mediated autophagy, however, has not been studied.

In the present study, we thus hypothesized that morphine via the induction of ER stress and subsequent initiation of autophagy ultimately culminates into astrocyte activation. To validate this, we examined the expression profiles of ER stress and autophagy signaling pathway markers, intracellular autophagosome formation, measured the autophagic flux through microtubule-associated protein 1 light chain 3 (LC3) turnover and p62 degradation and the glial fibrillary acidic protein (GFAP) and proinflammatory cytokine expression levels in both human A172 astrocytoma cell line and human primary astrocytes following exposure to morphine. The *in vitro* findings were further validated in the brains of morphine-dependent rhesus macaques. Our results underscore the association of ER stress-mediated initiation of autophagy with astrocytosis and neuroinflammation, in morphine-exposed astrocytes. Furthermore, chronic morphine exposure of rhesus macaques also resulted in region-specific induction of ER stress-autophagy signaling that was associated with increased expression of GFAP and proinflammatory cytokines. Interventions aimed at blocking either the MOR or ER stress signaling could thus be developed as promising therapeutic targets for abrogating morphine-mediated astrocytosis.

Materials and methods

Reagents

Morphine sulfate (Sigma-Aldrich, M8777), naltrexone (Sigma-Aldrich, N3136), wortmannin (Sigma-Aldrich, W3144), sodium 4-phenylbutyrate (4-PBA; EMD Millipore Corporation, 567616), antibodies such as, beclin 1 (BECN1; Santa Cruz Biotechnology, sc-11427), goat anti-rabbit (Santa Cruz Biotechnology, sc-2004), goat anti-mouse (Santa Cruz Biotechnology, sc-2005), PERK (Santa Cruz Biotechnology, sc-13073), LC3 (Novus Biological Company, NB100-2220), BiP (BD Biosciences, 610979), p62 (BL International, PM045), GFAP (Sigma-Aldrich, G3893) were purchased from commercial vendors as mentioned.

Animal studies

Archival brain tissues from rhesus macaques were used. Briefly, four monkeys were injected (*i.m.*) with morphine at the dose of 6 mg/ kg body weight/ day for the first week, 9 mg/ kg body weight/ day for the second week followed by 12 mg/ kg body weight/ day of morphine

injection for the next 10 weeks. Three equally divided doses per day were injected into these monkeys. The control group of four other monkeys received an injection of saline for the same 12 weeks as the morphine injected groups three times per day. After 12 weeks of saline or morphine injection, the animals were sacrificed, and different brain regions were dissected namely frontal cortex, parietal cortex, occipital cortex, brain stem, hippocampus, striatum, thalamus and cerebellum for further experimentation. The homogenates of the brain regions were used for assessing the mRNA expression of the proinflammatory cytokines (*TNF*, *IL1 β* , and *IL6*). Among the different brain areas, the frontal cortex, occipital cortex, brainstem, striatum, and cerebellum were used to determine the levels of ER stress and autophagic marker proteins, and GFAP immunostaining.

Cell culture

The human astrocytoma cell line A172 (ATCC® CRL1620TM - American Type Culture Collection) were cultured in Dulbecco's modified Eagle's medium (DMEM; Corning Cellgro®, 10-013-CV) containing 10 % heat-inactivated fetal bovine serum (FBS; Atlanta Biologicals, S11050H), penicillin-streptomycin (100 units/ml) (Life Technologies, 15140-122) in a 5% CO₂-humidified incubator at 37°C and the cells were used for up to 25 passages. Human primary astrocytes were obtained from ScienCell Research Laboratories (1800) and were cultured in astrocyte Media with 2% FBS (ScienCell Research Laboratories, 0010), 1% astrocyte growth supplement (ScienCell Research Laboratories, 1852) and 1% penicillin-streptomycin solution (ScienCell Research Laboratories, 0503) in a 5% CO₂-humidified incubator at 37°C. Human primary astrocytes were used up to 10 passages as per the manufacturer's protocol. The seeding densities of the human primary astrocytes, as well as the A172 astrocytoma cell line, were the same. Both the cell types were serum starved for 3 h before exposure to morphine.

Small interfering RNA (siRNA) transfection

Human A172 astrocytoma cell line and human primary astrocytes were seeded in 6-well plates (3×10^5 cells per well) and incubated overnight at 37°C in a humidified, 5% CO₂ incubator. Next day, cells were transfected with either human *BECN1* siRNA (Santa Cruz Biotechnology, sc-29797) or human *PERK* siRNA (Santa Cruz Biotechnology, sc-36213) by using Lipofectamine® 2000 Reagent (Life Technologies, 11668-019) as per the manufacturer's instructions. In brief, 1 ml of culture medium was replaced with 1 ml of Opti-MEM® | Reduced Serum Medium (Life Technologies, 31985-070) at 70% confluence. Meanwhile, Lipofectamine® 2000 Reagent (1 μ l/ml) and 120 pmol/ml of individually targeted siRNA were incubated separately with OptiMEM® I Reduced Serum Medium at room temperature for 5 min. Thereafter, the Lipofectamine® 2000 mix was added to the individually targeted siRNA mix, and this mixture was incubated for 20 min at room temperature, and subsequently, this mixture was added to the cells. Similarly, the scrambled siRNA mixture was also prepared. Thereafter, the culture plate was gently shaken for 5 s and incubated for 24 h in a humidified, 5% CO₂ incubator at 37°C. Knockdown efficiencies were confirmed by western blotting.

Autophagosome-lysosome fusion staining

Human A172 astrocytoma cell line and human primary astrocytes were seeded in a 24-well plate containing sterile glass coverslips (11 mm) at a density of 5×10^4 cells per well at 37°C in a humidified, 5% CO_2 incubator for 24 h. The cells were transfected with the RFP-GFP-LC3 plasmid (ptfLC3; Addgene plasmid # 21074) [54], using Lipofectamine® 2000 Reagent, according to the manufacturer's protocol, for 10 h following which the culture medium was replaced with the respective 10% heat-inactivated FBS-DMEM and the astrocytes were then treated with different agents. Thereafter, the astrocytes were rinsed 2 times with phosphate-buffered saline (PBS; Hyclone Laboratories, SH3025801) and fixed with 4% paraformaldehyde in PBS for 15 min at room temperature, followed by 3 times rinse with PBS. Subsequently, the coverslips were mounted on glass slides with ProLong Gold Antifade Reagent with DAPI (Molecular Probes, P36935). Fluorescent images were taken on a Zeiss Observer using a Z1 inverted microscope (Carl Zeiss, Thornwood, NY, USA) and the acquired images were analyzed using the AxioVs 40 Version 4.8.0.0 software (Carl Zeiss MicroImaging GmbH).

LC3 turnover and p62 degradation assay

Human A172 astrocytoma cell line was seeded in a 6-well plate at a density of 3×10^5 cells per well at 37°C in a humidified, 5% CO_2 incubator for 24 h. Next day cells were treated with either 500 nM of morphine or left untreated (control). Four hours before harvesting, the cells were treated with bafilomycin A1 (BAF; 400 nM; in control and morphine-exposed cells). These cells were processed further for western blot analysis of LC3 and p62.

Western blotting

The treated/transfected astrocytes and brain tissues from rhesus macaques were washed once with PBS and lysed using the Mammalian Cell Lysis kit (Sigma-Aldrich, MCL1-1KT). Cell lysates were centrifuged at $12000 \times g$ for 10 min at 4°C , the protein content of the supernatant was quantified by a BCA assay using Pierce™ BCA Protein Assay Kit (Thermo Fisher Scientific, 23227) according to the manufacturer's protocol. Equal amounts of soluble proteins were suspended in $5 \times$ Laemmli buffer and electrophoresed in a 10% or 15% sodium dodecyl sulfate-polyacrylamide gel and transferred onto a polyvinylidene fluoride membrane (Millipore, IPVH00010). After blocking of the membrane with 5% nonfat dry milk (in $1 \times$ TTBS buffer) for 1 h at room temperature, the membranes were incubated overnight with the primary antibodies at 4°C followed by incubation with secondary antibody the next day for 1 h at room temperature, and the immunoreactive protein signals were identified using Super Signal West Pico (Thermo Fisher Scientific, 34078) or Dura Chemiluminescent Substrate (Thermo Fisher Scientific, 34076). Image J (v1.4.3.67; NIH, Bethesda, MD) software was used for quantification [55]. Normalization was done with β -actin, an internal control and the fold change was obtained.

Real-Time qPCR

Total RNA was isolated from the cultured human astrocytes and different regions of rhesus macaques brain tissues using Quick-RNA™ MicroPrep kit (Zymo Research Corporation, R1051) as per the manufacturer's protocol. 1 μg of total RNA was used for the synthesis of

complementary DNA as described previously [37]. The reverse transcribed RNA was analyzed with the 7500 Fast Real-Time PCR System (Applied Biosystems, Grand Island, NY) with the RT² SYBR Green Fluor qPCR Mastermix (Qiagen, 330510). The primer sequences, for human astrocytes are - *TNF* forward 5'-CAGCCTCTTCTCCTTCCTGAT-3', *TNF* reverse 5'-GCCAGAGGGCTGATTAGAGA-3', *IL6* forward 5'-GATGAGTACAAAAGTCCTGATCCA-3', *IL6* reverse 5'-CTGCAGCCACTGGTTCTGT-3', *GAPDH* forward 5'-TGCACCACCAACTGCTTAGC-3', *GAPDH* reverse 5'-ATGCCAGTGAGCTTCCCGTT-3' and the primer sequences, for macaques are - *TNF* forward 5'-CCTCTTCAAGGGCCAAGGCT-3', *TNF* reverse 5'-GTCTGGTAGGAGACGGCGAT-3', *IL1β* forward 5'-TCAGCACCTCTCAAGCGGAA-3', *IL1β* reverse 5'-AATTGCATGGTGAAGTCAGT-3', *IL6* forward 5'-GAAGCTGCAGGCACAGAACC-3', *IL6* reverse 5'-CTGCAGCCACTGGTTCTGT-3', *GAPDH* forward 5'-CAGGCTGGACTGCAGGA-3', *GAPDH* reverse 5'-ATGACCTTGCCCACAGCCTT-3'. Each reaction was carried out in triplicate, and 4 independent experiments were run. Normalization was done with *GAPDH*, an internal control and the fold change in expression was obtained. The specificity of the qPCR was controlled using a non-template control.

ELISA

Human primary astrocytes (3×10^5 cells per well) were seeded onto 6 well plates and incubated overnight at 37°C in a humidified, 5% CO₂ incubator. Next day, after 3 h of serum starvation, cells were treated with 500 nM of morphine, and cell lysates as well as cell supernatants were collected following 3, 6, 12, 24 and 48 h of treatment and assessed for the detection of IL6 by ELISA using a human IL6 ELISA kit (Abcam; ab46027) according to the manufacturer's instructions.

Immunocytochemistry

Cells were seeded on the cover-slips (11 mm) in a 24-well plate at a density of 5×10^4 cells per well at 37°C in a humidified, 5% CO₂ incubator for 24h. Serum-starved astrocytes were exposed with morphine (500 nM) for 24 h. The astrocytes were next rinsed with 1× PBS and fixed with 4% paraformaldehyde in PBS for 20 min at room temperature, followed by permeabilization with 0.3% Triton X-100 (Fisher Scientific, BP151–500) in PBS and blocking in bovine serum albumin for 1 h at room temperature. Next, the cells were incubated overnight with appropriate primary antibody (1:200) at 4°C followed by incubation with secondary antibody Alexa Fluor 594 conjugated goat anti-rabbit IgG (H+L) for 2 h to detect the expression of the indicated protein. Thereafter, the coverslips were mounted on glass slides with ProLong Gold Antifade Reagent with DAPI (Molecular Probes, P36935). Fluorescence images were captured on a Zeiss Observer using a Z1 inverted microscope (Carl Zeiss, Thornwood, NY, USA) and the acquired images were analyzed using the AxioVs 40 Version 4.8.0.0 software (Carl Zeiss MicroImaging GmbH). Quantification was performed by Image J Launcher software.

Immunohistochemistry

Formalin-fixed paraffin-embedded tissue sections of different brain regions of saline administered and morphine-dependent rhesus macaques (each group n=4) were deparaffinized and rehydrated using a decreasing percentage of ethanol. Antigen retrieval was performed by boiling the slides in 0.01 M Tris-EDTA buffer, pH 9, for 20 min followed by incubation with 10% goat serum in PBS for 1 h at room temperature. Brain sections (5 μ m) were incubated with GFAP primary antibody overnight at 4°C. Secondary Alexa Fluor Alexa Fluor 488 goat anti-mouse was added for 2 h, followed by mounting with DAPI. Fluorescent images were acquired with Zeiss Observer. A Z1 inverted microscope; images were processed using AxioVs 40 Version 4.8.0.0 software. Densitometric scanning for GFAP staining was performed by Image J software.

Statistical analysis

The data are represented as mean \pm SEM. Non-parametric Kruskal-Wallis One-way ANOVA followed by Dunn's post hoc test was employed to compare the multiple experimental groups, and Wilcoxon matched-pairs signed rank test was used to compare between two groups using the GraphPad Prism software (Version 5). For the rhesus macaque study, Student's t test was used for comparing between two groups using the GraphPad Prism software (Version 5). Statistical analysis where probability levels were less than 0.05 were considered statistically significant.

Results

Morphine activates astrocytes and increases the expression of proinflammatory cytokines in human astrocytes

We initially sought to determine whether exposure of both the human A172 astrocytoma cell line, a transformed cell line, as well as human primary astrocytes (HPA), to morphine, could lead to astrocyte activation. Since astrocyte activation primarily depends on the concentration and exposure time of the stimulus, it was important first to ascertain the dose and time of morphine exposure leading to increased astrocyte activation. Cells were exposed to morphine at varying concentrations such as 0.125, 0.25, 0.5, 1, and 10 μ M for 24 h for assessing the expression of GFAP by western blotting. As shown in Figure 1A and 1B, morphine dose-dependently (0.25 to 10 μ M) increased the expression of GFAP in both human A172 astrocytoma cell line as well as HPA with a maximal expression at 500 nM. A concentration of 500 nM morphine was thus chosen for subsequent experiments. This concentration of morphine was in keeping with the physiological levels of morphine found in the postmortem brain tissues of narcotic overdose individuals (200 ng/g of brain tissue) [56]. Next, we sought to determine the optimal time of morphine-mediated induction of GFAP expression in human astrocytes exposed to morphine. Cells were exposed to morphine (500 nM) for the indicated time periods, such as 0, 3, 6, 12, 24 and 48 h, and assessed the expression of GFAP. As shown in Figure 1C and 1D, morphine time-dependently induced the expression of GFAP both in human A172 astrocytoma cell line (maximum expression at 24 h) and in HPA (maximum expression at 12 h). From the dose- and time-course studies, we determined 500 nM morphine as an optimal dose for both human A172 astrocytoma cell line and HPA, and 24 h as an optimal time for human A172

astrocytoma cell line, and 12 h, as an optimal time for HPA. Next, we wanted to examine the expression of GFAP in both human A172 astrocytoma and HPA exposed to 500 nM morphine for the indicated times by immunostaining. As shown in Figure 1E to 1H and as expected, morphine exposure notably induced the GFAP expression both in A172 astrocytoma cell line and HPA. Having confirmed that morphine-mediated astrocytosis, we next sought to examine the morphine-mediated production of proinflammatory cytokines in astrocytes. As shown in Figure 1I and 1J, morphine-exposed human A172 astrocytoma cell line and HPA significantly ($P<0.05$) increased the mRNA expression of proinflammatory cytokines, such as *TNF* and *IL6* in a time-dependent manner. Validation of these findings was also done by assessing protein levels of IL6 in both cell lysates and culture supernatants collected from morphine exposed astrocytes. As shown in Supplementary Fig.1A and 1B, morphine exposure resulted in a significant time-dependent increase of IL6 levels, thereby underscoring morphine-mediated activation of astrocytes.

Morphine induces ER stress and autophagy in human astrocytes

Several studies underscore the role of ER stress/autophagy axis in astrogliosis and neuroinflammation [37,57,58]. Morphine has also been shown to induce autophagy both in microglia and in neuroblastoma cell line [52,53]. Similarly, we next examined whether exposure of the human A172 cell line and HPA to morphine induces autophagy markers, such as BECN1, LC3-II, and p62. As shown in Figure 2A to 2F, morphine exposure resulted in the initiation of autophagy as indicated by increased expression of autophagy markers such as BECN1 (Fig. 2A and 2B), LC3-II (Fig. 2C and 2D). Intriguingly, morphine exposure also resulted in increased expression of p62 (Fig. 2E and 2F), indicating thereby defective autophagy in both human A172 astrocytoma and HPA. Importantly, as shown in Figure 2E and 2F, it was also shown that the expression levels of p62, a marker for autophagy flux, were time-dependently increased following morphine exposure in both human A172 astrocytoma cell line and HPA, thereby indicating a defective autophagic flux. Morphine-mediated initiation of autophagy was further validated by immunocytochemistry which demonstrated an increased staining for LC3 puncta in morphine-exposed cells, thereby confirming the initiation of autophagy and formation of autophagosome in the presence of morphine (Fig. 2G to 2J). Based on the fact that ER stress can induce autophagy, we next sought to assess the expression levels of the ER stress marker, binding Ig protein (BiP), an ER chaperone that is central to proper ER functioning, in morphine-exposed human A172 astrocytoma cell line and HPA. As shown in Figure 2K and 2L, morphine time-dependently increased the protein expression levels of BiP in both human A172 astrocytoma cell line and HPA thereby confirming the morphine-mediated induction of ER stress in these cells.

Morphine decreases the autophagic flux in human astrocytes

Since morphine-induces autophagosome formation in both the human A172 astrocytoma cell line and HPA, we next sought to determine whether the accumulation of autophagosomes was due to increased upstream activation of autophagy or rather, due to a blockade of autophagosome-lysosomal fusion. To determine this, we next measured the autophagic flux using the LC3 turnover assay and p62 degradation assay in astrocytes treated with morphine. p62 is a ubiquitin-binding adaptor protein that is selectively integrated into the phagophores by directly binding to the LC3 protein which, aids in the

turnover of ubiquitinated proteins, while itself getting degraded by autophagy. Increased accumulation of p62 protein is thus an indicator of autophagic flux inhibition inside the cell. Human A172 astrocytoma cell line was exposed to 500 nM morphine followed by treatment of cells with BAF - an inhibitor of autophagosome-lysosome fusion that was added at a saturating concentration of 400 nM during the last 4 h prior to cell harvesting. The cells were then assessed for the accumulation of LC3-II and p62 proteins. As shown in Figure 3A and 3B, exposure of human A172 astrocytoma cell line to 500 nM morphine followed by treatment with BAF significantly increased the accumulation of LC3-II/p62 proteins compared with control cells. Interestingly, similar to BAF-treated astrocytes, there was also an increased accumulation of LC3-II/ p62 in human A172 astrocytoma cell line treated with morphine alone, likely underscoring morphine-mediated decrease of the autophagic flux.

We next wanted to validate morphine-mediated inhibition of autophagic flux in human A172 astrocytoma cell line and HPA using the tandem fluorescent-tagged LC3 reporter plasmid transfection. Cells transfected with tandem fluorescent-tagged LC3 plasmid, having normal autophagosome formation express both RFP (red) and GFP (green) tagged LC3, but upon fusion with the lysosome, (due to the acidic pH) the GFP degrades, and predominantly RFP is expressed (Fig. 3C). Cells were transfected with a tandem fluorescent-tagged LC3 plasmid, followed by exposure of cells to either 500 nM morphine or BAF (400 nM) or 10 nM rapamycin, and subsequently assessed for the presence of red and green fluorescent LC3 puncta by immunofluorescence imaging. Compared to the control astrocytes, morphine exposure significantly increased the formation of red and green LC3 puncta in both human A172 astrocytoma cell line (Fig. 3D to 3F) and HPA (Fig. 3G and 3I). Treatment of astrocytes with BAF resulted in the formation of yellow puncta, which was comparable to the morphine alone group in both cell types. On the other hand, rapamycin (an autophagy inducer) treated astrocytes demonstrated significantly increased red puncta, indicating efficient fusion of autophagosomes with the lysosomes.

Morphine-mediated autophagy involves upstream activation of ER stress in human astrocytes

We next sought to determine if a link existed between autophagy and the upstream activation of ER stress. Herein cells were pretreated with either wortmannin (100 nM), a pharmacological inhibitor of autophagy (inhibitor of the PI3K signaling), for 1h or transfected with *BECN1* siRNA (gene silencing) followed by exposure to 500 nM morphine and assessed for expression of BECN1, LC3-II, and p62. As expected, pretreatment of human A172 astrocytoma cell line with wortmannin significantly inhibited the expression of autophagy markers (BECN1-Fig. 4A and LC3-II-Fig. 4B) with no change in p62 levels (Fig. 4C), and this was accompanied by abrogation of morphine-mediated induction of GFAP (Fig. 4D) and mRNA expression of proinflammatory cytokines such as *TNF* and *IL6* (Fig. 4E). Interestingly, however, pretreatment with wortmannin had no effect on the expression of ER stress sensor protein – BiP, indicating thereby that the ER stress response was upstream of autophagy in morphine-treated human A172 astrocytoma cell line (Fig. 4F).

These findings were further validated using the gene silencing approach (*BECN1* siRNA transfection). Both the human A172 astrocytoma cell line and HPA were transfected with

either *BECN1* siRNA or scrambled siRNA, followed by exposure to 500 nM morphine and assessed for expression of autophagy and ER stress markers by western blotting. As expected, in *BECN1* siRNA transfected human A172 astrocytoma cell line morphine failed to induce autophagy, as evidenced by the decreased expression levels of BECN1 (Fig. 4G), LC3-II (Fig. 4H), and p62 (Fig. 4I) compared with scrambled siRNA transfected astrocytes. Conversely, the protein levels of ER stress sensor protein- BiP remained significantly higher in *BECN1* siRNA transfected human A172 astrocytoma cell line exposed to morphine compared with the scrambled siRNA transfected cells without any treatment (Fig. 4J). On the other hand, and as expected, morphine failed to induce the expression of downstream GFAP protein (Fig. 4K), and mRNA expression of proinflammatory cytokines (Fig. 4L) in *BECN1* siRNA transfected cells compared to scrambled siRNA transfected cells. Also, as expected, a similar trend was found in *BECN1* siRNA transfected HPA exposed to morphine compared to scrambled siRNA-transfected cells exposed to morphine (Fig. 4M to 4R).

Based on our findings that morphine exposure resulted in upstream ER stress activation leading to initiation of autophagy, we next wanted to investigate the effect of blocking ER stress on both ER stress and autophagy markers in morphine-treated human astrocytes. Human A172 astrocytoma cell line was pretreated with 50 μ M 4-PBA for 1 h (a chaperone-like ER stress inhibitor, which binds with the hydrophobic domain of misfolded proteins thereby blocking their aggregation [59]), followed by exposure to morphine (500 nM) and assessed for the expression of ER stress marker (BiP), autophagy markers (BECN1, LC3-II and p62), astrocyte activation marker (GFAP) and mRNA expression of proinflammatory cytokines (*TNF* and *IL6*). Interestingly, morphine failed to induce the expression of BiP (Fig. 5A) as well as the autophagy markers, such as BECN1 (Fig. 5B), LC3-II (Fig. 5C), and p62 (Fig. 5D) in human A172 astrocytoma cell line pretreated with the ER stress inhibitor, 4-PBA. In parallel, morphine also failed to induce the expression of GFAP (Fig. 5E) and proinflammatory cytokines (Fig. 5F) in cells pretreated with 4-PBA.

These findings were next validated using a gene silencing approach, i.e., transfection of cells with *PERK* siRNA. The rationale for silencing *PERK* gene is that ER stress-mediated by PERK signaling arm sequentially phosphorylates the eIF2 α , which subsequently results in repression of global protein synthesis, thereby preventing the unfolded protein load in the ER [60]. Herein both the human A172 astrocytoma cell line and HPA were transfected with either *PERK* or scrambled siRNAs followed by exposure to morphine (500 nM) and assessed for expression of PERK and BiP, autophagy markers (BECN1, LC3-II and p62) and the astrocyte activation marker (GFAP) by western blotting and also assessed for mRNA expression of proinflammatory cytokines (*TNF* and *IL6*) by qPCR. As expected in *PERK* siRNA transfected human A172 astrocytoma cell line, morphine exposure failed to induce the ER stress markers (PERK- Fig. 5G and BiP -Fig. 5H), autophagy markers, such as BECN1 (Fig. 5I), LC3-II (Fig. 5J), and p62 (Fig. 5K), astrocyte activation marker, GFAP (Fig. 5L), as well as mRNA expression of proinflammatory cytokines, such as *TNF* and *IL6* (Fig. 5M). Intriguingly, we found a similar trend in *PERK* siRNA transfected HPA exposed to 500 nM morphine (Figure 5N to 5T). Overall, these data provided evidence that in human astrocytes exposed to morphine, activation of ER stress was upstream of autophagy.

Morphine-mediated defective autophagy involves μ -opioid receptor (MOR) in astrocytes

Next, we sought to explore whether in astrocytes morphine-mediated defective autophagy involved MOR. To confirm this, astrocytes were pretreated with MOR antagonist naltrexone (100 μ M) for 1 h prior to morphine exposure and assessed for the expression of markers for ER stress, autophagy, GFAP and proinflammatory cytokines. Pretreatment of human A172 astrocytoma cell line with 100 μ M naltrexone (for 1 h) followed by 500 nM morphine treatment, resulted in statistically significant ($P<0.05$) decrease in the expression of ER stress markers such as BiP (Fig. 6A), autophagy markers such as, BECN1 (Fig. 6B), LC3-II (Fig. 6C), astrocyte activation marker, GFAP (Fig. 6D) and mRNA expression of proinflammatory cytokines, such as *TNF* and *IL6* (Fig. 6E) compared to the astrocytes exposed to morphine alone. Similar results were obtained in HPA pretreated with 100 μ M naltrexone for 1 h followed by 500 nM morphine exposure for another 24 h (Fig. 6F to 6J). Taken together, these results demonstrated evidence for the upstream involvement of MOR in morphine-mediated defective autophagy, leading in turn, to astrocyte activation and production of proinflammatory cytokines.

Morphine-dependent rhesus macaques exert brain region-specific upregulation of proinflammatory cytokines.

To validate our *in vitro* findings *in vivo*, we next sought to determine the region-specific expression of proinflammatory cytokines in the archived brain tissues, of morphine-dependent rhesus macaques. As expected, in the archived brain tissues of chronically administered morphine there was significantly ($P<0.05$) increased mRNA expression of proinflammatory cytokines (*TNF*, *IL1 β* , and *IL6*) in the frontal cortex (Fig. 7A), occipital cortex (Fig. 7B), basal ganglia (Fig. 7C) and the cerebellum (Fig. 7D). In contrast, the mRNA expression of these proinflammatory cytokines was significantly ($P<0.05$) decreased in regions such as the parietal cortex (Fig. 7E), hippocampus (Fig. 7F) and brainstem (Fig. 7G). The thalamus (Fig. 7H) showed no change in mRNA expression of the proinflammatory cytokines in the two groups of macaques. These findings thus demonstrated brain-region specific upregulation of proinflammatory cytokines in morphine-dependent rhesus macaques compared with the saline administered controls.

Morphine-dependent rhesus macaques exhibit brain region-specific activation of astrocytes

Next, we wanted to correlate the astrocyte activation status in the different brain regions of morphine-dependent macaques that exhibited changes in mRNA expression of proinflammatory cytokines (*TNF*, *IL1 β* , and *IL6*) and compare this with the saline administered rhesus macaques. Interestingly, expression of the astrocyte activation marker, GFAP correlated with the same regions that demonstrated increased expression of proinflammatory cytokines (frontal cortex-Fig. 8A; occipital cortex-Fig. 8B; basal ganglia-Fig. 8C; the granular cell layer (Fig. 8D) as well as the cerebellar white matter (Fig. 8E) of morphine-dependent rhesus macaques compared with the saline-administered group. The expression of GFAP in the brain stem of morphine-dependent rhesus macaques, however, was significantly decreased compared with that of the saline-administered group (Fig. 8F).

Figure 8G demonstrates the quantification of GFAP expression in all the brain regions (Fig. 8G)

Morphine-dependent rhesus macaques exert brain region-specific activation of astrocytes through ER stress and defective autophagy

Based on the *in vitro* findings demonstrating the role of the ER stress-autophagy signaling axis in morphine-mediated induction of astrocyte activation and generation of proinflammatory cytokines, we next sought to assess the expression of ER stress and autophagy marker proteins in the frontal cortex, occipital cortex, basal ganglia, cerebellum and the brain stem of morphine-dependent and saline administered rhesus macaques. Interestingly, and as expected, morphine-dependent rhesus macaques exhibited significantly increased expression of ER stress sensor protein, BiP (Fig. 9A) and autophagy markers, BECN1 (Fig. 9B), LC3-II (Fig. 9C) and p62 (Fig. 9D) in the frontal cortex compared with saline administered rhesus macaques. Similarly, in the occipital cortex BiP (Fig. 9E), BECN1 (Fig. 9F), LC3-II (Fig. 9G) and p62 (Fig. 9H) expressions were significantly increased ($P<0.05$) in morphine-dependent compared with saline controls. In the cerebellum also, morphine-dependent animals exhibited significantly ($P<0.05$) increased expression of BiP (Fig. 9I) and the autophagy markers, BECN1 (Fig. 9J) and LC3-II (Fig. 9K); expression of p62 (Fig. 9L) however, remained unchanged compared with saline controls. On the other hand, in the basal ganglia, expression of ER stress marker BiP (Fig. 9M) was significantly increased, while the expression of autophagy markers, BECN1 (Fig. 9N), LC3-II (Fig. 9O) and p62 (Fig. 9P) remained unchanged in morphine-dependent rhesus macaques compared with saline controls. Intriguingly, in the brainstem of morphine-dependent macaques, expression of BiP (Fig. 9Q) remained unchanged while the expression of autophagy markers, BECN1 (Fig. 9R), LC3-II (Fig. 9S) and p62 (Fig. 9T) was downregulated compared with saline controls. Taken together, these results showed brain region-specific activation of ER stress and defective autophagy signaling in morphine-dependent rhesus macaques compared with the saline-administered group. Further, these data are in line with the *in vitro* findings and thus underscore the role of ER stress-mediated defective autophagy in morphine-induced astrocytosis.

Discussion

Morphine is the most commonly used painkiller in the clinical setting [1]. Chronic use of morphine, however, leads to various ill effects including drug tolerance, addiction, and cognitive impairment [9]. Several studies have implicated the role of morphine in inducing neuronal injury and apoptosis [43,16], impairing microglial chemotaxis [15], and inducing microglial activation [61]. The effects of morphine on astrocytes, especially in the context of ER-stress-mediated defective autophagy, however, have not been reported. In the present study, we demonstrated that in astrocytes morphine-mediated induction of GFAP expression involved the ER stress-mediated defective autophagy axis, subsequently leading to the generation of proinflammatory cytokines. Consistent with our results, morphine exposure resulted in increased astrocyte activation with upregulation of GFAP expression. Similar upregulation of GFAP has also been observed in neuropathic pain [20], during morphine tolerance [21], and in HIV-1 infection of the CNS [62]. Morphine exposure of human

astrocytes also increased the expression levels of proinflammatory cytokines (*TNF* and *IL6*). Interestingly, morphine has also been shown to induce neuroinflammation in the brain endothelial cells through activation of Toll-like receptor 4 (TLR4) signaling [63].

Morphine has been shown to induce autophagy in the neuroblastoma cell line [52], in bone marrow-derived macrophages [64], and in the mice hippocampus [2,65,52,43]. Our previous studies have also shown that morphine exposure resulted in synaptic injury in the hippocampal neurons and that this was mediated via the ER stress-autophagy axis [43]. The present study demonstrates that in astrocytes morphine exposure results in initiation of autophagy as well as autophagosome formation. Additionally, we found that defective autophagy was primarily mediated by incomplete fusion of autophagosomes with the lysosome. This was evidenced by the increased formation of yellow puncta in morphine-exposed human astrocytes, and, these findings were in line with that observed in BAF-treated astrocytes, thereby confirming morphine-mediated defective fusion of autophagosomes with lysosomes. These results were further confirmed using the LC3 turnover assay and p62 degradation assay in astrocytes. In support of our findings, similar findings have also been shown in other cell types by other groups. For example, in bone marrow-derived macrophages, morphine exposure increased lipopolysaccharide-mediated autophagy but inhibited autophagosome formation thereby leading to decreased bacterial clearance and increased bacterial load through TLR4 signaling [64]. It has also been reported that exposure of human pulmonary microvascular endothelial cells to both the HIV-1 Tat protein and morphine resulted in an oxidative stress-dependent increased expression of autophagy markers and increased generation of autophagosomes compared to cells exposed to either agent alone. Intriguingly, treatment of these cells with morphine alone or in combination with HIV-1 Tat inhibited the fusion of autophagosome with the lysosomes [66]. Induction of autophagy by morphine is cell-type specific. For example, there are reports that morphine exposure to either microglia or neurons failed to induce autophagy [67,53]. It has been shown from several studies that defective autophagy could play a role in the generation of proinflammatory cytokines. For example, studies have shown that macrophages isolated from Atg1611 knockout mice produced more IL-1 β following stimulation with lipopolysaccharide, an effect mediated by excessive activation of caspase-1 via the adapter molecule, Toll-like receptor adaptor molecule 1 [68]. It has also been shown that induction of autophagy can lead to inactivation of nuclear factor- κ B (NF- κ B) via selective degradation of BCL10 complexes [69]. Reciprocally then, defective autophagy leading to increased activation of NF- κ B could result in increased inflammation. Defects in autophagy have been found by genetic association studies to confer susceptibility to several autoimmune and inflammatory disorders, particularly inflammatory bowel disease [70]. A possible explanation for the block in fusion of autophagosome with the lysosomes could be attributed to either the loss of lysosomal acidification and/or loss of lysosomal proteases, thereby leading to accumulation of autophagosomes inside the cells [71–73]. In our study, we found increased accumulation of autophagosomes that was accompanied by defective lysosomal fusion, in astrocytes exposed to morphine.

Emerging data suggest a possible interplay between ER stress and the induction of autophagy [46]. Additionally, several studies have demonstrated that initiation of autophagy acts as a survival mechanism in cells exposed to ER stress and that the survival response is

specifically induced to trigger the initiation of autophagosome formation [49,74–76]. It has also been reported that the eIF2 α /ATF4 pathway plays a key role in regulation of autophagy via the induction of Atg12 expression [76,77]. Under ER stress conditions, PERK - one of the regulators of ER stress regulates autophagy genes by increasing the transcription of a set of genes implicated in the formation, elongation and function of the autophagosome [76]. An additional mechanism that regulates ER stress mediated autophagy, is via ER-stress mediated release of Ca²⁺ into the cytosol, which, in turn, leads to activation of various kinases and proteases involved in autophagy signaling [76,78,79]. Recent reports however, suggest the regulatory role of PERK-mediated ER stress marker and the activation of autophagy in different CNS cells such as the neurons [49,46,80], microglia [50,81], and astrocytes [37,57]. Accordingly, the present study also showed that morphine-mediated autophagy was mediated by upregulation of PERK and was validated using both the pharmacological inhibitors as well as the gene silencing approach. More specifically, the pharmacological inhibitors of autophagy signaling, such as wortmannin and the genetic approach involving transfection of astrocytes with *BECN1* siRNA followed by morphine exposure resulted in inhibition of morphine-mediated autophagy, astrocyte activation and induction of proinflammatory cytokines with no effect on the expression of ER stress markers. Intriguingly, pretreatment of A172 astrocytes with the ER stress inhibitor, 4-PBA or transfection of human astrocytes with *PERK* siRNA resulted in inhibition of morphine-induced ER stress, autophagy, astrocyte activation as well as expression of proinflammatory cytokines, thereby confirming that ER stress markers lie upstream of autophagy. The present findings are in agreement with our previous report demonstrating that morphine-induced ER stress/autophagy axis was critical for synaptic impairment in hippocampal neurons [43]. Taken together, our *in vitro* data showed that morphine induces ER stress-mediated defective autophagy which, in turn, leads to astrocyte activation and secretion of proinflammatory cytokines. The role of morphine-mediated activation of ER stress has been reported previously in the *in vivo* morphine tolerance [82,83].

We further validated the cell culture findings in the archival brain tissues from morphine-dependent rhesus macaques. In the *in vivo* study, we observed differential effects that were region-specific in the brains of morphine-dependent macaques. Chronic administration of morphine (for up to 12 weeks) to the rhesus macaques resulted in increased expression of proinflammatory cytokines in the frontal cortex, occipital cortex, cerebellum and basal ganglia, and decreased expression in the hippocampus, parietal cortex, and brainstem compared with the saline administered animals. No change was observed in the thalamus of the two groups of macaques. These findings are in keeping with the previous reports wherein morphine administered rats exhibited neuroinflammation in the cortex [84,85], nucleus accumbens [86], ventral tegmental area [87], and cerebellum [85], and decreased expression of proinflammatory cytokines in the rat hippocampus [88], and brain stem [86]. Interestingly, morphine-dependent animals exhibited increased proinflammatory cytokines expression in brain regions (frontal cortex, occipital cortex, cerebellum and basal ganglia) where the ER stress-mediated defective autophagy was predominant. In contrast, decreased autophagy and decreased expression of proinflammatory cytokines was observed in the brain stem of morphine-dependent rhesus macaques compared with the saline group. These results

are in agreement with the findings reported by other investigators showing morphine-mediated induction of autophagy in the rat brains [43,52].

In addition to increased activation of ER stress signaling and defective autophagy and upregulation of proinflammatory cytokines in the brain regions, such as frontal cortex, occipital cortex, cerebellum and basal ganglia of morphine-dependent rhesus macaques, concomitantly we also found increased expression of the astrocyte activation marker GFAP, in the same brain regions. There was dampened astrocyte activation in the brain stem of morphine-dependent rhesus macaques compared with that of saline. Intriguingly, in the morphine-dependent macaques, the brain regions (parietal cortex, brainstem, and thalamus) that failed to exhibit increased autophagy and astrocytosis were also the regions involved in nociception, while, in contrast, the regions not associated with nociception demonstrated increased impairment of autophagy and increased astrocytosis. A possible explanation for this could be that in the nociceptive regions of the brain, that harbor increased numbers of opioid receptors, morphine actually plays a protective role by dampening astrocytosis. Our findings are in agreement with those of Johnson *et al.*, wherein the authors reported similar regional effects of morphine with increased astrocytosis in brain areas unrelated to nociception [87].

In summary, our findings have demonstrated that morphine induces ER stress-mediated defective autophagy, which in turn, leads to astrocytosis and neuroinflammation via the MOR. The present study for the first time showed brain region-specific effects of chronic morphine administration in rhesus macaques. In line with our *in vitro* findings, the *in vivo* data also demonstrated the role of morphine-induced ER stress-mediated defective autophagy in astrocyte activation and proinflammatory cytokines expression in the frontal cortex, occipital cortex, cerebellum and basal ganglia region of macaque brains. This study has unraveled specific molecular pathways critical for morphine-induced astrocytosis, which, in the future, could be critical for the development of interventions aimed at abrogating morphine-mediated astrocyte activation. Findings from these studies could also inform the clinicians about the adverse cognitive effects of opioid, thereby limiting their use.

Supplementary Material

Refer to Web version on PubMed Central for supplementary material.

Acknowledgements

This work was supported by grants DA033614, DA035203, and DA041751 (SB) from the National Institutes of Health. We are grateful to Drs. Guoku Hu, Ernest Chivero, Annadurai Thangaraj, and Mr. Ke Liao for their useful discussions and to Ms. Fang Niu and Ms. Yeon Hee Kook for their technical assistance.

References

1. Stefano GB, Ptacek R, Kuzelova H, Kream RM (2012) Endogenous morphine: up-to-date review 2011. *Folia biologica* 58 (2):49–56 [PubMed: 22578954]
2. Johnson F, Setnik B (2011) Morphine sulfate and naltrexone hydrochloride extended-release capsules: naltrexone release, pharmacodynamics, and tolerability. *Pain physician* 14 (4):391–406 [PubMed: 21785483]

3. Ting S, Schug S (2016) The pharmacogenomics of pain management: prospects for personalized medicine. *J Pain Res* 9:49–56. doi:10.2147/JPR.S55595 [PubMed: 26929662]
4. Morizio KM, Baum RA, Dugan A, Martin JE, Bailey AM (2017) Characterization and Management of Patients with Heroin versus Nonheroin Opioid Overdoses: Experience at an Academic Medical Center. *Pharmacotherapy*. doi:10.1002/phar.1902
5. Friedman H, Eisenstein TK (2004) Neurological basis of drug dependence and its effects on the immune system. *J Neuroimmunol* 147 (1–2):106–108 [PubMed: 14741438]
6. Roy S, Wang J, Kelschenbach J, Koodie L, Martin J (2006) Modulation of immune function by morphine: implications for susceptibility to infection. *J Neuroimmune Pharmacol* 1 (1):77–89. doi: 10.1007/s11481-005-9009-8 [PubMed: 18040793]
7. Roy S, Barke RA, Loh HH (1998) MU-opioid receptor-knockout mice: role of muopioid receptor in morphine mediated immune functions. *Brain Res Mol Brain Res* 61 (1–2):190–194 [PubMed: 9795212]
8. Roy S, Ninkovic J, Banerjee S, Charboneau RG, Das S, Dutta R, Kirchner VA, Koodie L, Ma J, Meng J, Barke RA (2011) Opioid drug abuse and modulation of immune function: consequences in the susceptibility to opportunistic infections. *J Neuroimmune Pharmacol* 6 (4):442–465. doi: 10.1007/s11481-011-9292-5 [PubMed: 21789507]
9. Chau DL, Walker V, Pai L, Cho LM (2008) Opiates and elderly: use and side effects. *Clinical interventions in aging* 3 (2):273–278 [PubMed: 18686750]
10. Roy S, Chapin RB, Cain KJ, Charboneau RG, Ramakrishnan S, Barke RA (1997) Morphine inhibits transcriptional activation of IL-2 in mouse thymocytes. *Cell Immunol* 179 (1):1–9. doi: 10.1006/cimm.1997.1147 [PubMed: 9259765]
11. Roy S, Cain KJ, Charboneau RG, Barke RA (1998) Morphine accelerates the progression of sepsis in an experimental sepsis model. *Adv Exp Med Biol* 437:21–31 [PubMed: 9666253]
12. Dinda A, Gitman M, Singhal PC (2005) Immunomodulatory effect of morphine: therapeutic implications. *Expert Opin Drug Saf* 4 (4):669–675. doi:10.1517/14740338.4.4.669 [PubMed: 16011446]
13. Liu HC, Anday JK, House SD, Chang SL (2004) Dual effects of morphine on permeability and apoptosis of vascular endothelial cells: morphine potentiates lipopolysaccharide-induced permeability and apoptosis of vascular endothelial cells. *J Neuroimmunol* 146 (1–2):13–21 [PubMed: 14698842]
14. Wen H, Lu Y, Yao H, Buch S (2011) Morphine induces expression of platelet-derived growth factor in human brain microvascular endothelial cells: implication for vascular permeability. *PLoS One* 6 (6):e21707. doi:10.1371/journal.pone.0021707 [PubMed: 21738771]
15. Hu S, Chao CC, Hegg CC, Thayer S, Peterson PK (2000) Morphine inhibits human microglial cell production of, and migration towards, RANTES. *Journal of psychopharmacology* 14 (3):238–243. doi:10.1177/026988110001400307 [PubMed: 11106302]
16. Hu S, Sheng WS, Lokensgard JR, Peterson PK (2002) Morphine induces apoptosis of human microglia and neurons. *Neuropharmacology* 42 (6):829–836 [PubMed: 12015209]
17. Horvath RJ, DeLeo JA (2009) Morphine enhances microglial migration through modulation of P2X4 receptor signaling. *The Journal of neuroscience : the official journal of the Society for Neuroscience* 29 (4):998–1005. doi:10.1523/JNEUROSCI.4595-08.2009
18. Hauser KF, Stiene-Martin A, Mattson MP, Elde RP, Ryan SE, Godleske CC (1996) mu-Opioid receptor-induced Ca²⁺ mobilization and astroglial development: morphine inhibits DNA synthesis and stimulates cellular hypertrophy through a Ca²⁺-dependent mechanism. *Brain research* 720 (1–2):191–203. doi:10.1016/0006-8993(96)00103-5 [PubMed: 8782912]
19. Bruce-Keller AJ, Turchan-Cholewo J, Smart EJ, Geurin T, Chauhan A, Reid R, Xu R, Nath A, Knapp PE, Hauser KF (2008) Morphine causes rapid increases in glial activation and neuronal injury in the striatum of inducible HIV-1 Tat transgenic mice. *Glia* 56 (13):1414–1427. doi: 10.1002/glia.20708 [PubMed: 18551626]
20. Tawfik VL, LaCroix-Fralish ML, Natile-McMenemy N, DeLeo JA (2005) Transcriptional and translational regulation of glial activation by morphine in a rodent model of neuropathic pain. *The Journal of pharmacology and experimental therapeutics* 313 (3):1239–1247. doi:10.1124/jpet.104.082420 [PubMed: 15743926]

21. Di Cesare Mannelli L, Corti F, Micheli L, Zanardelli M, Ghelardini C (2015) Delay of morphine tolerance by palmitoylethanolamide. *BioMed research international* 2015:894732. doi: 10.1155/2015/894732 [PubMed: 25874232]
22. Childers SR, Snyder SH (1978) Guanine nucleotides differentiate agonist and antagonist interactions with opiate receptors. *Life Sci* 23 (7):759–761 [PubMed: 211364]
23. Childers SR, Creese I, Snowman AM, Synder SH (1979) Opiate receptor binding affected differentially by opiates and opioid peptides. *Eur J Pharmacol* 55 (1):11–18 [PubMed: 220062]
24. Diaz A, Ruiz F, Florez J, Pazos A, Hurlle MA (1995) Regulation of dihydropyridine-sensitive Ca⁺⁺ channels during opioid tolerance and supersensitivity in rats. *J Pharmacol Exp Ther* 274 (3):1538–1544 [PubMed: 7562531]
25. Diaz A, Florez J, Pazos A, Hurlle MA (2000) Opioid tolerance and supersensitivity induce regional changes in the autoradiographic density of dihydropyridine-sensitive calcium channels in the rat central nervous system. *Pain* 86 (3):227–235 [PubMed: 10812252]
26. Nestler EJ (1996) Under siege: The brain on opiates. *Neuron* 16 (5):897–900 [PubMed: 8630245]
27. Ippolito DL, Temkin PA, Rogalski SL, Chavkin C (2002) N-terminal tyrosine residues within the potassium channel Kir3 modulate GTPase activity of Galphai. *J Biol Chem* 277 (36):32692–32696. doi:10.1074/jbc.M204407200 [PubMed: 12082117]
28. Torrecilla M, Quillinan N, Williams JT, Wickman K (2008) Pre- and postsynaptic regulation of locus coeruleus neurons after chronic morphine treatment: a study of GIRK-knockout mice. *Eur J Neurosci* 28 (3):618–624. doi:10.1111/j.1460-9568.2008.06348.x [PubMed: 18702733]
29. Wickman K, Clapham DE (1995) Ion channel regulation by G proteins. *Physiol Rev* 75 (4):865–885. doi:10.1152/physrev.1995.75.4.865 [PubMed: 7480165]
30. Torrecilla M, Marker CL, Cintora SC, Stoffel M, Williams JT, Wickman K (2002) G-protein-gated potassium channels containing Kir3.2 and Kir3.3 subunits mediate the acute inhibitory effects of opioids on locus ceruleus neurons. *J Neurosci* 22 (11):4328–4334. doi:20026414 [PubMed: 12040038]
31. Volterra A, Meldolesi J (2005) Astrocytes, from brain glue to communication elements: the revolution continues. *Nature reviews Neuroscience* 6 (8):626–640. doi:10.1038/nrn1722 [PubMed: 16025096]
32. Abbott NJ, Ronnback L, Hansson E (2006) Astrocyte-endothelial interactions at the blood-brain barrier. *Nature reviews Neuroscience* 7 (1):41–53. doi:10.1038/nrn182 [PubMed: 16371949]
33. Hadera MG, Eloqayli H, Jaradat S, Nehlig A, Sonnewald U (2015) Astrocyteneuronal interactions in epileptogenesis. *Journal of neuroscience research* 93 (7):1157–1164. doi:10.1002/jnr.23584 [PubMed: 25782696]
34. Wang DD, Bordey A (2008) The astrocyte odyssey. *Progress in neurobiology* 86 (4):342–367. doi: 10.1016/j.pneurobio.2008.09.015 [PubMed: 18948166]
35. Yan X, Shi ZF, Xu LX, Li JX, Wu M, Wang XX, Jia M, Dong LP, Yang SH, Yuan F (2017) Glutamate Impairs Mitochondria Aerobic Respiration Capacity and Enhances Glycolysis in Cultured Rat Astrocytes. *Biomedical and environmental sciences : BES* 30 (1):44–51. doi:10.3967/bes2017.005 [PubMed: 28245898]
36. Hostenbach S, Cambron M, D’Haeseleer M, Kooijman R, De Keyser J (2014) Astrocyte loss and astrogliosis in neuroinflammatory disorders. *Neuroscience letters* 565:39–41. doi:10.1016/j.neulet.2013.10.012 [PubMed: 24128880]
37. Periyasamy P, Guo ML, Buch S (2016) Cocaine induces astrocytosis through ER stress-mediated activation of autophagy. *Autophagy* 12 (8):1310–1329. doi:10.1080/15548627.2016.1183844 [PubMed: 27337297]
38. Guilarte TR, Nihei MK, McGlothan JL, Howard AS (2003) Methamphetamine-induced deficits of brain monoaminergic neuronal markers: distal axotomy or neuronal plasticity. *Neuroscience* 122 (2):499–513 [PubMed: 14614914]
39. Narita M, Suzuki M, Kuzumaki N, Miyatake M, Suzuki T (2008) Implication of activated astrocytes in the development of drug dependence: differences between methamphetamine and morphine. *Annals of the New York Academy of Sciences* 1141:96–104. doi:10.1196/annals.1441.032 [PubMed: 18991953]

40. Slezak M, Korostynski M, Gieryk A, Golda S, Dzbek J, Piechota M, Wlazlo E, Bilecki W, Przewlocki R (2013) Astrocytes are a neural target of morphine action via glucocorticoid receptor-dependent signaling. *Glia* 61 (4):623–635. doi:10.1002/glia.22460 [PubMed: 23339081]
41. Lazriev IL, Kiknadze GI, Kutateladze II, Nebieridze MI (2001) Effect of morphine on the number and branching of astrocytes in various regions of rat brain. *Bulletin of experimental biology and medicine* 131 (3):248–250 [PubMed: 11427911]
42. Ikeda H, Miyatake M, Koshikawa N, Ochiai K, Yamada K, Kiss A, Donlin MJ, Panneton WM, Churchill JD, Green M, Siddiqui AM, Leinweber AL, Crews NR, Ezerskiy LA, Rendell VR, Belcheva MM, Coscia CJ (2010) Morphine modulation of thrombospondin levels in astrocytes and its implications for neurite outgrowth and synapse formation. *The Journal of biological chemistry* 285 (49):38415–38427. doi:10.1074/jbc.M110.109827 [PubMed: 20889977]
43. Cai Y, Yang L, Hu G, Chen X, Niu F, Yuan L, Liu H, Xiong H, Arikath J, Buch S (2016) Regulation of morphine-induced synaptic alterations: Role of oxidative stress, ER stress, and autophagy. *J Cell Biol* 215 (2):245–258. doi:10.1083/jcb.201605065 [PubMed: 27810915]
44. Kim KH, Lee MS (2014) Autophagy--a key player in cellular and body metabolism. *Nat Rev Endocrinol* 10 (6):322–337. doi:10.1038/nrendo.2014.35 [PubMed: 24663220]
45. Ryter SW, Cloonan SM, Choi AM (2013) Autophagy: a critical regulator of cellular metabolism and homeostasis. *Molecules and cells* 36 (1):7–16. doi:10.1007/s10059-013-0140 [PubMed: 23708729]
46. Senft D, Ronai ZA (2015) UPR, autophagy, and mitochondria crosstalk underlies the ER stress response. *Trends in biochemical sciences* 40 (3):141–148. doi:10.1016/j.tibs.2015.01.002 [PubMed: 25656104]
47. Lindholm D, Wootz H, Korhonen L (2006) ER stress and neurodegenerative diseases. *Cell death and differentiation* 13 (3):385–392. doi:10.1038/sj.cdd.4401778 [PubMed: 16397584]
48. Cai Y, Arikath J, Yang L, Guo ML, Periyasamy P, Buch S (2016) Interplay of endoplasmic reticulum stress and autophagy in neurodegenerative disorders. *Autophagy* 12 (2):225–244. doi:10.1080/15548627.2015.1121360 [PubMed: 26902584]
49. Ogata M, Hino S, Saito A, Morikawa K, Kondo S, Kanemoto S, Murakami T, Taniguchi M, Tanii I, Yoshinaga K, Shiosaka S, Hammarback JA, Urano F, Imaizumi K (2006) Autophagy is activated for cell survival after endoplasmic reticulum stress. *Molecular and cellular biology* 26 (24):9220–9231. doi:10.1128/MCB.01453-06 [PubMed: 17030611]
50. Guo ML, Liao K, Periyasamy P, Yang L, Cai Y, Callen SE, Buch S (2015) Cocaine-mediated microglial activation involves the ER stress-autophagy axis. *Autophagy* 11 (7):995–1009. doi:10.1080/15548627.2015.1052205 [PubMed: 26043790]
51. Roy S, Cain KJ, Chapin RB, Charboneau RG, Barke RA (1998) Morphine modulates NF kappa B activation in macrophages. *Biochemical and biophysical research communications* 245 (2):392–396. doi:10.1006/bbrc.1998.8415 [PubMed: 9571161]
52. Zhao L, Zhu Y, Wang D, Chen M, Gao P, Xiao W, Rao G, Wang X, Jin H, Xu L, Sui N, Chen Q (2010) Morphine induces Beclin 1- and ATG5-dependent autophagy in human neuroblastoma SH-SY5Y cells and in the rat hippocampus. *Autophagy* 6 (3):386–394 [PubMed: 20190558]
53. El-Hage N, Rodriguez M, Dever SM, Masvekar RR, Gewirtz DA, Shacka JJ (2015) HIV-1 and morphine regulation of autophagy in microglia: limited interactions in the context of HIV-1 infection and opioid abuse. *Journal of virology* 89 (2):1024–1035. doi:10.1128/JVI.02022-14 [PubMed: 25355898]
54. Kimura S, Noda T, Yoshimori T (2007) Dissection of the autophagosome maturation process by a novel reporter protein, tandem fluorescent-tagged LC3. *Autophagy* 3 (5):452–460 [PubMed: 17534139]
55. Schneider CA, Rasband WS, Eliceiri KW (2012) NIH Image to ImageJ: 25 years of image analysis. *Nature methods* 9 (7):671–675 [PubMed: 22930834]
56. Pare EM, Monforte JR, Thibert RJ (1984) Morphine concentrations in brain tissue from heroin-associated deaths. *Journal of analytical toxicology* 8 (5):213–216 [PubMed: 6094915]
57. Yu B, Wenjun Z, Changsheng Y, Yuntao F, Jing M, Ben L, Hai Q, Guangwei X, Suhua W, Fang L, Aschner M, Rongzhu L (2016) Preconditioning of endoplasmic reticulum stress protects against

acrylonitrile-induced cytotoxicity in primary rat astrocytes: The role of autophagy.

Neurotoxicology 55:112–121. doi:10.1016/j.neuro.2016.05.020 [PubMed: 27260289]

58. Cao L, Walker MP, Vaidya NK, Fu M, Kumar S, Kumar A (2016) Cocaine-Mediated Autophagy in Astrocytes Involves Sigma 1 Receptor, PI3K, mTOR, Atg5/7, Beclin-1 and Induces Type II Programed Cell Death. *Mol Neurobiol* 53 (7):4417–4430. doi:10.1007/s12035-015-9377-x [PubMed: 26243186]
59. Kubota K, Niinuma Y, Kaneko M, Okuma Y, Sugai M, Omura T, Uesugi M, Uehara T, Hosoi T, Nomura Y (2006) Suppressive effects of 4-phenylbutyrate on the aggregation of Pael receptors and endoplasmic reticulum stress. *J Neurochem* 97 (5):1259–1268. doi:10.1111/j.1471-4159.2006.03782.x [PubMed: 16539653]
60. Rozpedek W, Pytel D, Mucha B, Leszczynska H, Diehl JA, Majsterek I (2016) The Role of the PERK/eIF2alpha/ATF4/CHOP Signaling Pathway in Tumor Progression During Endoplasmic Reticulum Stress. *Curr Mol Med* 16 (6):533–544 [PubMed: 27211800]
61. Fukagawa H, Koyama T, Kakuyama M, Fukuda K (2013) Microglial activation involved in morphine tolerance is not mediated by toll-like receptor 4. *Journal of anesthesia* 27 (1):93–97. doi:10.1007/s00540-012-1469-4 [PubMed: 22926420]
62. Tauber SC, Staszewski O, Prinz M, Weis J, Nolte K, Bunkowski S, Bruck W, Nau R (2016) HIV encephalopathy: glial activation and hippocampal neuronal apoptosis, but limited neural repair. *HIV Med* 17 (2):143–151. doi:10.1111/hiv.12288 [PubMed: 26176591]
63. Wang X, Loram LC, Ramos K, de Jesus AJ, Thomas J, Cheng K, Reddy A, Somogyi AA, Hutchinson MR, Watkins LR, Yin H (2012) Morphine activates neuroinflammation in a manner parallel to endotoxin. *Proceedings of the National Academy of Sciences of the United States of America* 109 (16):6325–6330. doi:10.1073/pnas.1200130109 [PubMed: 22474354]
64. Wan J, Ma J, Anand V, Ramakrishnan S, Roy S (2015) Morphine potentiates LPS-induced autophagy initiation but inhibits autophagosomal maturation through distinct TLR4-dependent and independent pathways. *Acta physiologica* 214 (2):189–199. doi:10.1111/apha.12506 [PubMed: 25850855]
65. Pan Y, Sun X, Jiang L, Hu L, Kong H, Han Y, Qian C, Song C, Qian Y, Liu W (2016) Metformin reduces morphine tolerance by inhibiting microglial-mediated neuroinflammation. *Journal of neuroinflammation* 13 (1):294. doi:10.1186/s12974-016-0754-9 [PubMed: 27855689]
66. Dalvi P, Sharma H, Chinnappan M, Sanderson M, Allen J, Zeng R, Choi A, O'Brien-Ladner A, Dhillon NK (2016) Enhanced autophagy in pulmonary endothelial cells on exposure to HIV-Tat and morphine: Role in HIV-related pulmonary arterial hypertension. *Autophagy* 12 (12):2420–2438. doi:10.1080/15548627.2016.1238551 [PubMed: 27723373]
67. Dever SM, Rodriguez M, Lapierre J, Costin BN, El-Hage N (2015) Differing roles of autophagy in HIV-associated neurocognitive impairment and encephalitis with implications for morphine co-exposure. *Frontiers in microbiology* 6:653. doi:10.3389/fmicb.2015.00653 [PubMed: 26217309]
68. Saitoh T, Fujita N, Jang MH, Uematsu S, Yang BG, Satoh T, Omori H, Noda T, Yamamoto N, Komatsu M, Tanaka K, Kawai T, Tsujimura T, Takeuchi O, Yoshimori T, Akira S (2008) Loss of the autophagy protein Atg16L1 enhances endotoxin-induced IL-1beta production. *Nature* 456 (7219):264–268. doi:10.1038/nature0738 [PubMed: 18849965]
69. Paul S, Kashyap AK, Jia W, He YW, Schaefer BC (2012) Selective autophagy of the adaptor protein Bcl10 modulates T cell receptor activation of NF-kappaB. *Immunity* 36 (6):947–958. doi:10.1016/j.immuni.2012.04.008 [PubMed: 22658522]
70. Henckaerts L, Cleynen I, Brinar M, John JM, Van Steen K, Rutgeerts P, Vermeire S (2011) Genetic variation in the autophagy gene ULK1 and risk of Crohn's disease. *Inflamm Bowel Dis* 17 (6):1392–1397. doi:10.1002/ibd.21486 [PubMed: 21560199]
71. Nakamura S, Yoshimori T (2017) New insights into autophagosome-lysosome fusion. *J Cell Sci* 130 (7):1209–1216. doi:10.1242/jcs.196352 [PubMed: 28302910]
72. Button RW, Roberts SL, Willis TL, Hanemann CO, Luo S (2017) Accumulation of autophagosomes confers cytotoxicity. *The Journal of biological chemistry* 292 (33):13599–13614. doi:10.1074/jbc.M117.782276 [PubMed: 28673965]
73. Hori I, Otomo T, Nakashima M, Miya F, Negishi Y, Shiraiishi H, Nonoda Y, Magara S, Tohyama J, Okamoto N, Kumagai T, Shimoda K, Yukitake Y, Kajikawa D, Morio T, Hattori A, Nakagawa M,

- Ando N, Nishino I, Kato M, Tsunoda T, Saitsu H, Kanemura Y, Yamasaki M, Kosaki K, Matsumoto N, Yoshimori T, Saitoh S (2017) Defects in autophagosome-lysosome fusion underlie Vici syndrome, a neurodevelopmental disorder with multisystem involvement. *Sci Rep* 7 (1):3552. doi:10.1038/s41598-017-02840-8 [PubMed: 28615637]
74. Schroder M (2008) Endoplasmic reticulum stress responses. *Cell Mol Life Sci* 65 (6):862–894. doi:10.1007/s00018-007-7383-5 [PubMed: 18038217]
75. Kroemer G, Marino G, Levine B (2010) Autophagy and the integrated stress response. *Mol Cell* 40 (2):280–293. doi:10.1016/j.molcel.2010.09.023 [PubMed: 20965422]
76. B'Chir W, Maurin AC, Carraro V, Averous J, Jousse C, Muranishi Y, Parry L, Stepien G, Fafournoux P, Bruhat A (2013) The eIF2alpha/ATF4 pathway is essential for stress-induced autophagy gene expression. *Nucleic Acids Res* 41 (16):7683–7699. doi:10.1093/nar/gkt563 [PubMed: 23804767]
77. Kouroku Y, Fujita E, Tanida I, Ueno T, Isoai A, Kumagai H, Ogawa S, Kaufman RJ, Kominami E, Momoi T (2007) ER stress (PERK/eIF2alpha phosphorylation) mediates the polyglutamine-induced LC3 conversion, an essential step for autophagy formation. *Cell Death Differ* 14 (2):230–239. doi:10.1038/sj.cdd.4401984 [PubMed: 16794605]
78. Hoyer-Hansen M, Bastholm L, Szyniarowski P, Campanella M, Szabadkai G, Farkas T, Bianchi K, Fehrenbacher N, Elling F, Rizzuto R, Mathiasen IS, Jaattela M (2007) Control of macroautophagy by calcium, calmodulin-dependent kinase kinase-beta, and Bcl-2. *Mol Cell* 25 (2):193–205. doi:10.1016/j.molcel.2006.12.009 [PubMed: 17244528]
79. Yousefi S, Perozzo R, Schmid I, Ziemiecki A, Schaffner T, Scapozza L, Brunner T, Simon HU (2006) Calpain-mediated cleavage of Atg5 switches autophagy to apoptosis. *Nat Cell Biol* 8 (10):1124–1132. doi:10.1038/ncb1482 [PubMed: 16998475]
80. Liu S, Sarkar C, Dinizo M, Faden AI, Koh EY, Lipinski MM, Wu J (2015) Disrupted autophagy after spinal cord injury is associated with ER stress and neuronal cell death. *Cell Death Dis* 6:e1582. doi:10.1038/cddis.2014.527 [PubMed: 25569099]
81. Ye J, Jiang Z, Chen X, Liu M, Li J, Liu N (2017) The role of autophagy in pro-inflammatory responses of microglia activation via mitochondrial reactive oxygen species in vitro. *J Neurochem*. doi:10.1111/jnc.14042
82. Aoe T (2013) [Endoplasmic reticulum stress and opioid tolerance withdrawal]. *Masui The Japanese journal of anesthesiology* 62 (3):283–289 [PubMed: 23544329]
83. Dobashi T, Tanabe S, Jin H, Nishino T, Aoe T (2010) Valproate attenuates the development of morphine antinociceptive tolerance. *Neuroscience letters* 485 (2):125–128. doi:10.1016/j.neulet.2010.08.084 [PubMed: 20816918]
84. Ghavimi H, Hassanzadeh K, Maleki-Dizaji N, Azarfardian A, Ghasami S, Zolali E, Charkhpour M (2014) Pioglitazone prevents morphine antinociception tolerance and withdrawal symptoms in rats. *Naunyn-Schmiedeberg's archives of pharmacology* 387 (9):811–821. doi:10.1007/s00210-014-0996-y
85. Campbell LA, Avdoshina V, Rozzi S, Mocchetti I (2013) CCL5 and cytokine expression in the rat brain: differential modulation by chronic morphine and morphine withdrawal. *Brain, behavior, and immunity* 34:130–140. doi:10.1016/j.bbi.2013.08.006
86. Amaral GF, Dossa PD, Viebig LgB, Konno FTC, Consoli A, Martins MdFtM, Viani FvC, Bondan EF (2016) Astrocytic expression of GFAP and serum levels of IL-1² and TNF-± in rats treated with different pain relievers. *Brazilian Journal of Pharmaceutical Sciences* 52:623–633
87. Beitner-Johnson D, Guitart X, Nestler EJ (1993) Glial fibrillary acidic protein and the mesolimbic dopamine system: regulation by chronic morphine and Lewis-Fischer strain differences in the rat ventral tegmental area. *J Neurochem* 61 (5):1766–1773 [PubMed: 8228992]
88. Patel NA, Romero AA, Zadina JE, Chang SL (1996) Chronic exposure to morphine attenuates expression of interleukin-1 beta in the rat hippocampus. *Brain research* 712 (2):340–344 [PubMed: 8814911]

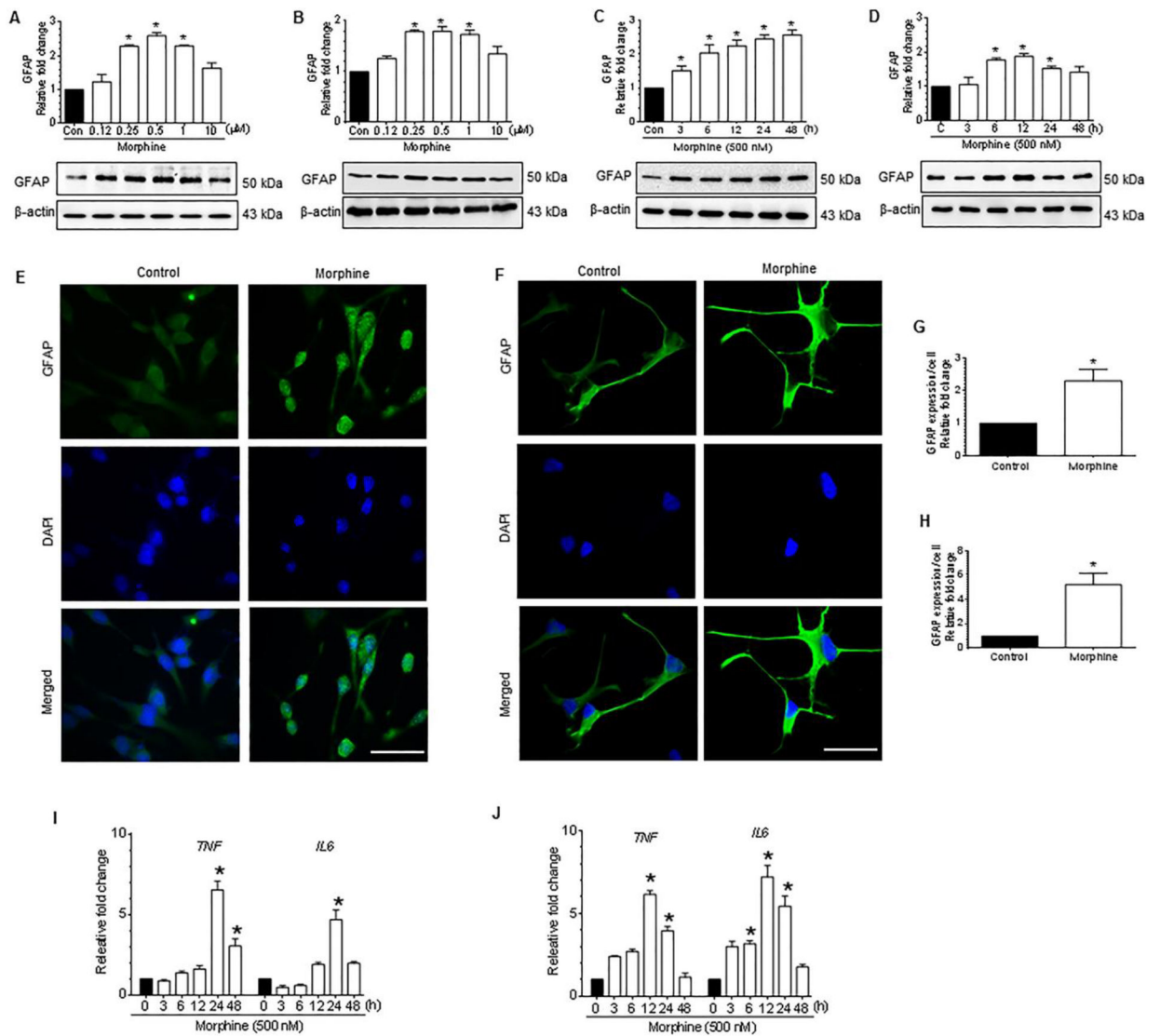


Figure 1. Morphine-mediated activation of astrocytes and secretion of proinflammatory cytokines in human astrocytes. (A and B) Representative western blots showing the dose-dependent upregulation of GFAP in human A172 astrocytoma cell line (A) and in HPA (B) exposed to varying doses of morphine ranging from 125 nM to 10 μ M for 24 h. (C and D) Representative western blots showing time-dependent upregulation of GFAP in human A172 astrocytoma cell line (C) and HPA (D) exposed to 500 nM morphine for the indicated time points. (E and F) Representative immunocytochemistry images confirming the upregulation of GFAP in human A172 astrocytoma cell line (E) and HPA (F) exposed to morphine (500 nM). Scale bar: 50 μ M. (G and H) Quantitative analysis of GFAP expression in human A172 astrocytoma cell line (G) and HPA (H) by densitometric scanning using Image J software. (I and J) qPCR analysis showing the time-dependent upregulation of proinflammatory cytokines, such as *TNF* and *IL6* in human A172 astrocytoma cell line (I) and HPA (J) exposed to 500 nM morphine. β -actin was used as a loading control for western blot and

GAPDH for mRNA expression of cytokines. Data are presented as mean \pm SEM; n = 6. Non-parametric Kruskal-Wallis One-way ANOVA followed by Dunn's *post hoc* test was used to determine the statistical significance between multiple groups and Wilcoxon matched-pairs signed rank test was used to compare between two groups: *, P < 0.05 vs. control.

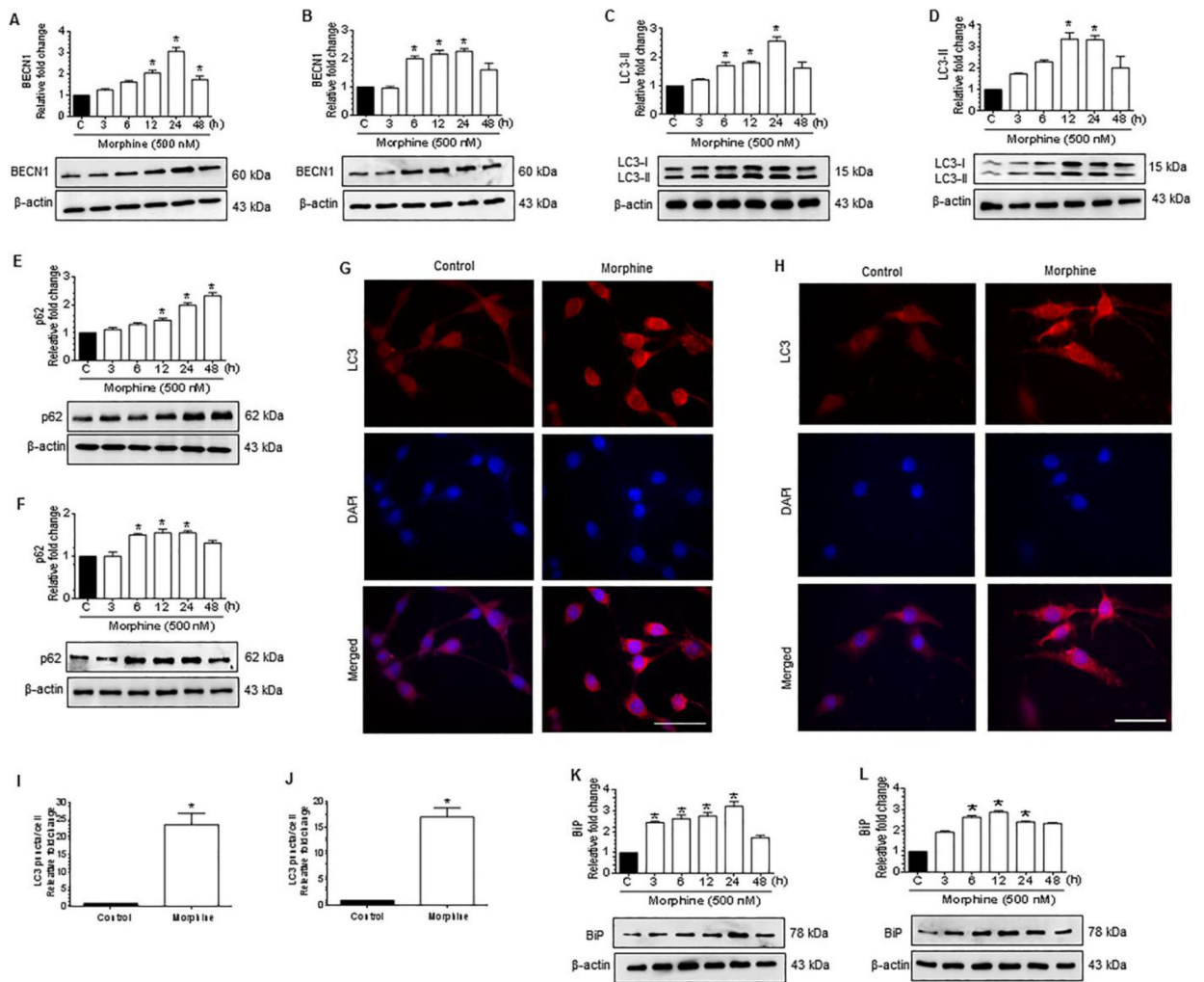


Figure 2. Morphine-mediated initiation of autophagy and ER stress in human astrocytes. (A and B) Representative western blots showing time-dependent upregulation of BECN1 in human A172 astrocytoma cell line (A) and HPA (B) exposed to morphine (500 nM) for the indicated time points. (C and D) Representative western blots showing time-dependent upregulation of LC3-II in human A172 astrocytoma cell line (C) and HPA (D) exposed to morphine (500 nM) for the indicated time points. (E and F) Representative western blots showing time-dependent upregulation of p62 in human A172 astrocytoma cell line (E) and HPA (F) exposed to morphine (500 nM) for the indicated time points. (G and H) Representative immunocytochemistry images confirming morphine-mediated upregulation of LC3 in human A172 astrocytoma cell line (G) and HPA (H) exposed to morphine (500 nM). Scale bar: 50 μ M. (I and J) Quantitative analysis of LC3 puncta formation in human A172 astrocytoma cell line (I) and HPA (J) exposed to morphine (500 nM). (K and L) Representative western blots showing time-dependent upregulation of BiP in human A172 astrocytoma cell line (K) and HPA (L) exposed to morphine (500 nM) for indicated time points. β -actin was used as a loading control for all experiments. Data are presented as mean \pm SEM; n = 6. Non-parametric Kruskal -Wallis One-way ANOVA followed by Dunn's *post*

hoc test was used to determine the statistical significance between multiple groups and Wilcoxon matched-pairs signed rank test was used to compare between two groups: *, $P < 0.05$ vs. control.

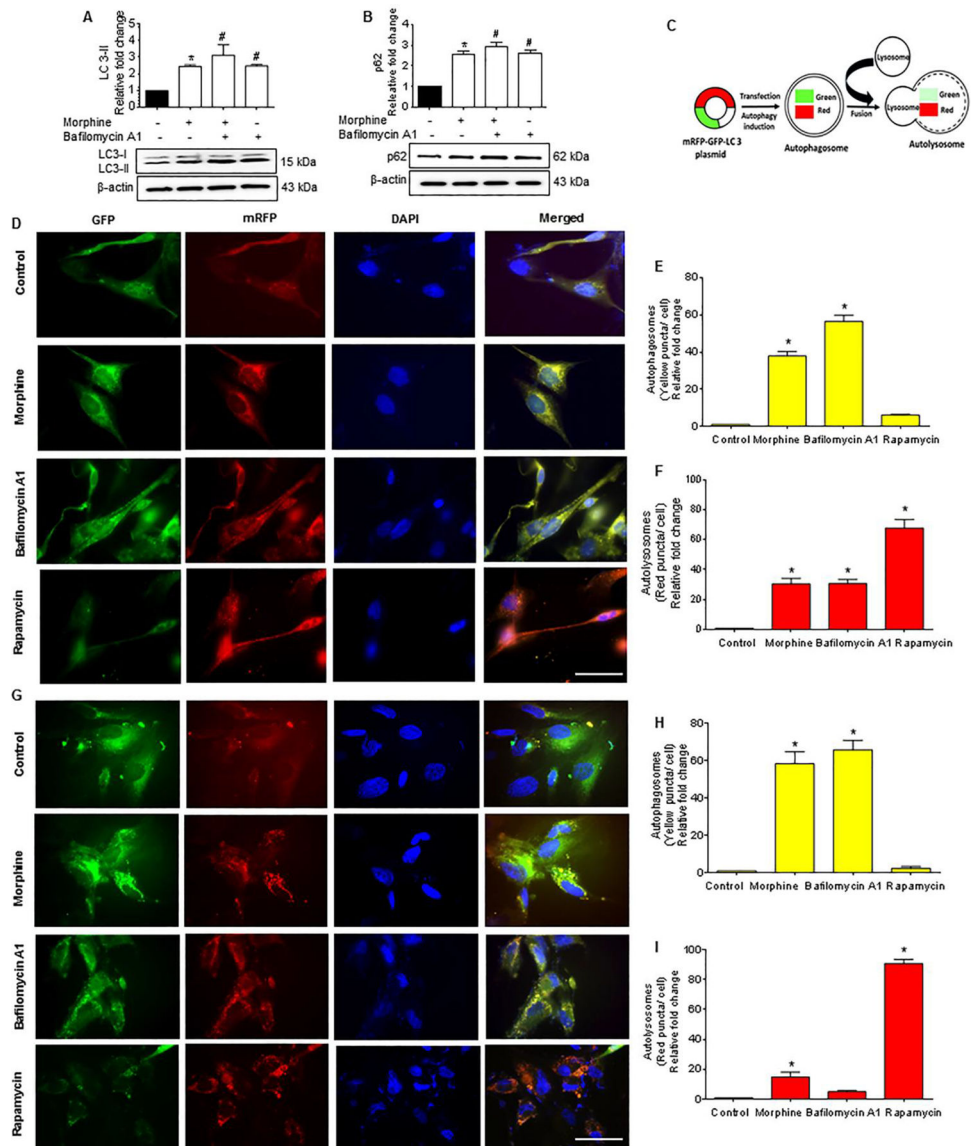


Figure 3. Morphine-mediated defective autophagy in human astrocytes. (A and B) Representative western blots showing protein levels of LC3-II (A) and p62 (B) in human A172 astrocytoma cell line exposed to morphine (500 nM) for 24 h followed by treatment with 400 nM BAF, which was added in the last 4 h of the 24 h treatment period. (C) Schematic representation of the mechanism of tandem fluorescent-tagged LC3 plasmid-mediated identification of the autophagosome fusion with the lysosome. (D) Representative fluorescent photomicrographs showing the LC3 puncta formation in human A172 astrocytoma cell line transfected with tandem fluorescent-tagged LC3 plasmid and treated with 500 nM morphine for 24 h, 400 nM BAF - last 4 h of the 24 h treatment period and 10 nM rapamycin for 24 h. (E and F) Quantitative analysis of yellow puncta (E) and red puncta (F) formation in different experimental groups of tandem fluorescent-tagged LC3 plasmid transfected human A172 astrocytoma cell line. (G) Representative fluorescent photomicrographs showing the LC3

puncta formation in HPA transfected with tandem fluorescent-tagged LC3 plasmid and treated with 500 nM morphine for 12 h, 400 nM BAF – last 4 h of the 12 h treatment period and 10 nM rapamycin for 12 h. (H and I) Quantitative analysis of yellow puncta (H) and red puncta (I) formation in different experimental groups of tandem fluorescent-tagged LC3 plasmid transfected HPA. Scale bar: 50 μ M. β -actin was used as a loading control for all experiments. Data are presented as mean \pm SEM; n = 6. Non-parametric Kruskal – Wallis One-way ANOVA followed by Dunn's *post hoc* test was used to determine the statistical significance between multiple groups and Wilcoxon test was used to compare between two groups: *, P<0.05 vs control; #, P<0.05 vs. morphine.

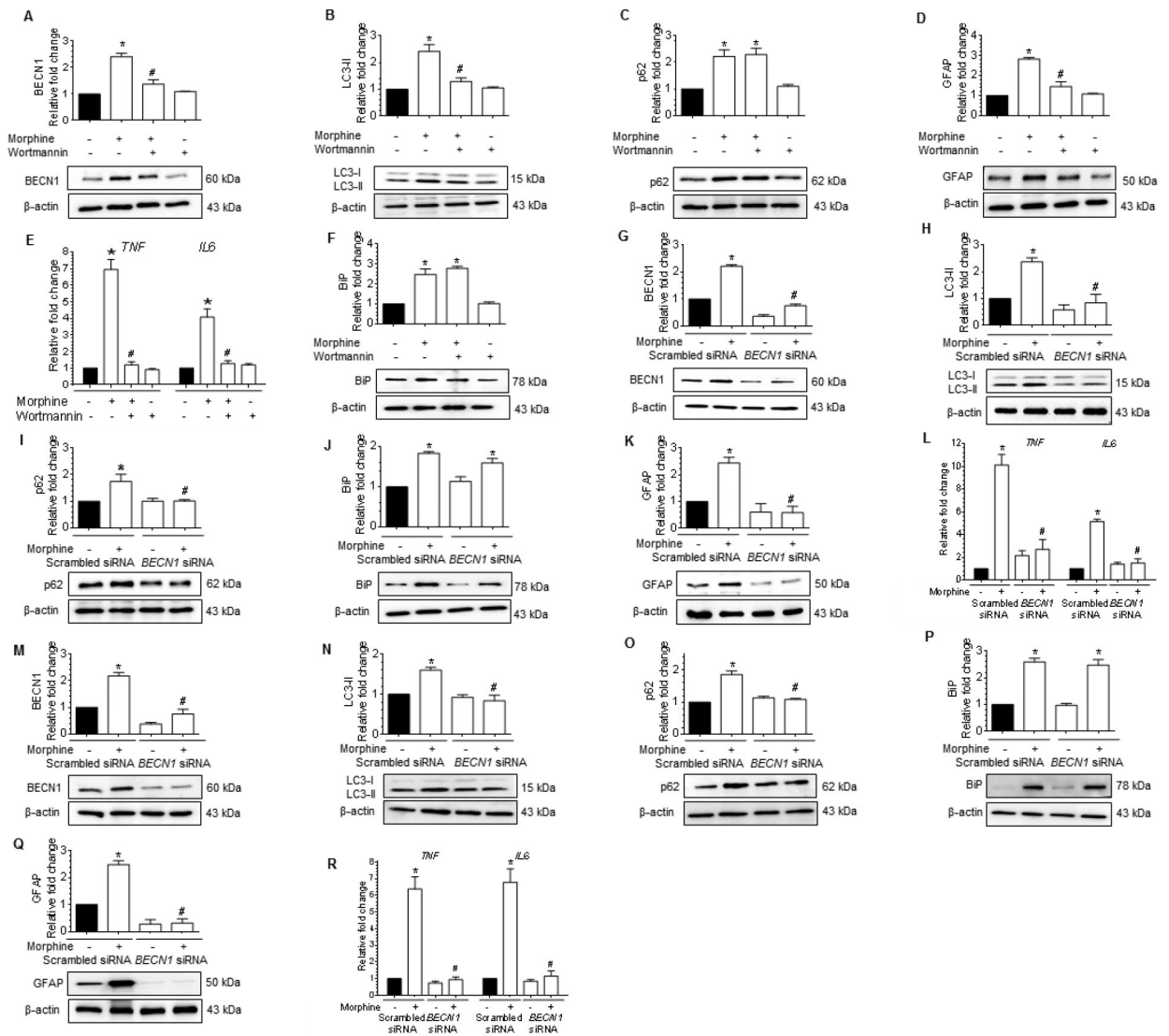


Figure 4. Morphine-mediated defective autophagy involves upstream activation of ER stress in human astrocytes. (A-D) Representative western blots showing the protein levels of BECN1 (A), LC3-II (B), p62 (C) and GFAP (D) in human A172 astrocytoma cell line pretreated with 100 nM wortmannin for 1 h followed by 500 nM morphine for 24 h. (E) qPCR showing relative expression of proinflammatory cytokines such as *TNF* and *IL6* mRNA, and (F) Representative western blot showing the expression of the BiP protein in human A172 astrocytoma cell line pretreated with 100 nM wortmannin for 1 h followed by 500 nM morphine for 24 h. (G-K) Representative western blots showing the protein levels of BECN1 (G), LC3-II (H), p62 (I), BiP (J) and GFAP (K) in human A172 astrocytoma cell line transfected with *BECN1* siRNA and scrambled siRNA followed by 500 nM morphine for 24 h. (L) qPCR showing the relative expression of proinflammatory cytokines such as *TNF* and *IL6* mRNA in human A172 astrocytoma cell line transfected with *BECN1* and scrambled siRNAs followed by 500 nM morphine for 24 h. (M-Q) Representative western blots showing protein levels of BECN1 (M), LC3-II (N), p62 (O), BiP (P) and GFAP (Q) in

human primary astrocytes transfected with *BECN1* and scrambled siRNAs followed by 500 nM morphine for 12 h. (R) qPCR showing the relative expression of proinflammatory cytokines such as *TNF* and *IL6* mRNA in human primary astrocytes transfected with *BECN1* and scrambled siRNAs followed by 500 nM morphine for 12 h. β -actin was used as a loading control for western blot and *GAPDH* for mRNA expression of cytokines. Data are presented as mean \pm SEM; n = 6. Non-parametric Kruskal-Wallis One-way ANOVA followed by Dunn's *post hoc* test was used to determine the statistical significance between multiple groups: *, P<0.05 vs. control; #, P<0.05 vs. morphine.

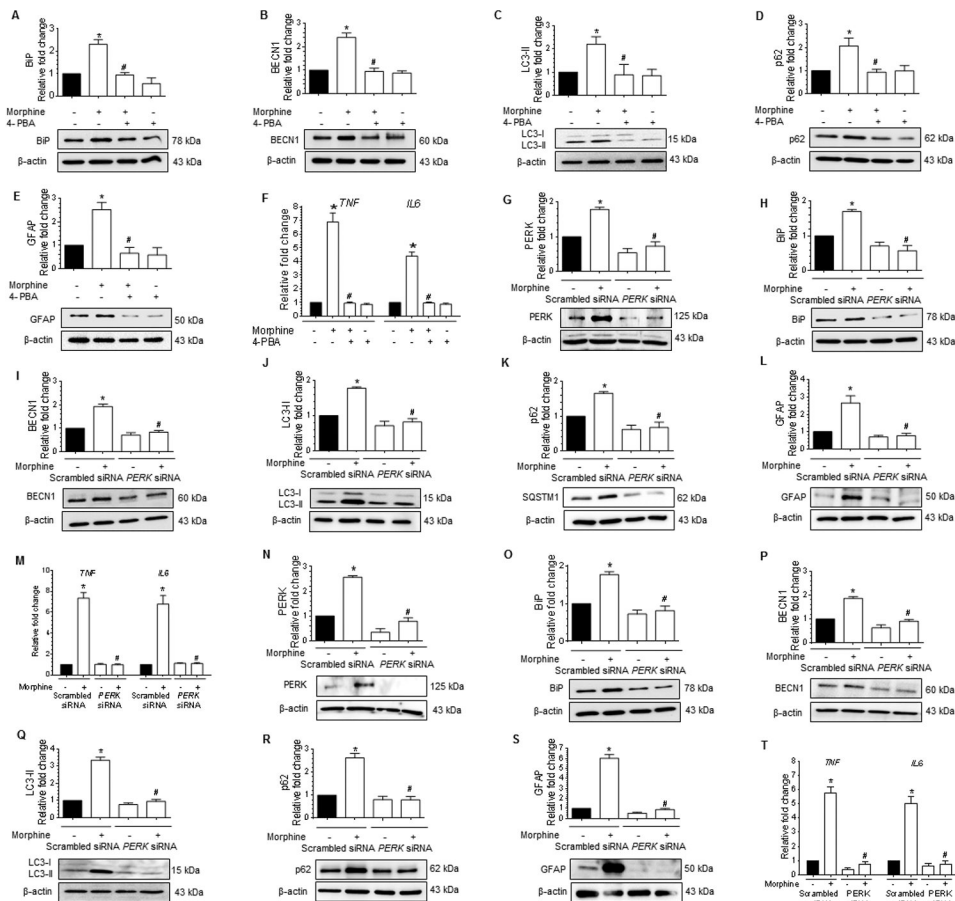


Figure 5. Morphine-mediated defective autophagy involves upstream activation of ER stress in human astrocytes. (A-E) Representative western blots showing the protein levels of BiP (A), BECN1 (B), LC3-II (C), p62 (D) and GFAP (E) in human A172 astrocytoma cell line pretreated with 50 μ M 4-PBA for 1 h followed by 500 nM morphine for 24 h. (F) qPCR showing the relative expression of proinflammatory cytokines such as *TNF* and *IL6* mRNA in human A172 astrocytoma cell line pretreated with 50 μ M 4-PBA for 1 h followed by 500 nM morphine for 24 h. (G-L) Representative western blots showing the protein levels of PERK (G), BiP (H), BECN1 (I), LC3-II (J), p62 (K), and GFAP (L) in human A172 astrocytoma cell line transfected with *PERK* and scrambled siRNAs followed by 500 nM morphine for 24 h. (M) qPCR showing the relative expression of proinflammatory cytokines such as *TNF* and *IL6* mRNA in human A172 astrocytoma cell line transfected with *PERK* and scrambled siRNAs followed by 500 nM morphine for 24 h. (N-T) Representative western blots showing the protein levels of PERK (N), BiP (O), BECN1 (P), LC3-II (Q), p62 (R), and GFAP (S) in human primary astrocytes transfected with *PERK* siRNA and scrambled siRNA followed by 500 nM morphine for 12 h. (T) qPCR showing the relative expression of proinflammatory cytokines such as *TNF* and *IL6* mRNA in human primary astrocytes transfected with *PERK* siRNA and scrambled siRNA followed by 500 nM morphine for 12 h. β -actin was used as a loading control for western blot and GAPDH for mRNA expression of cytokines. Data are presented as mean \pm SEM; n = 6. Non-parametric Kruskal-Wallis One-way ANOVA

followed by Dunn's *post hoc* test was used to determine the statistical significance between multiple groups: *, $P < 0.05$ vs. control; #, $P < 0.05$ vs. morphine.

Author Manuscript

Author Manuscript

Author Manuscript

Author Manuscript

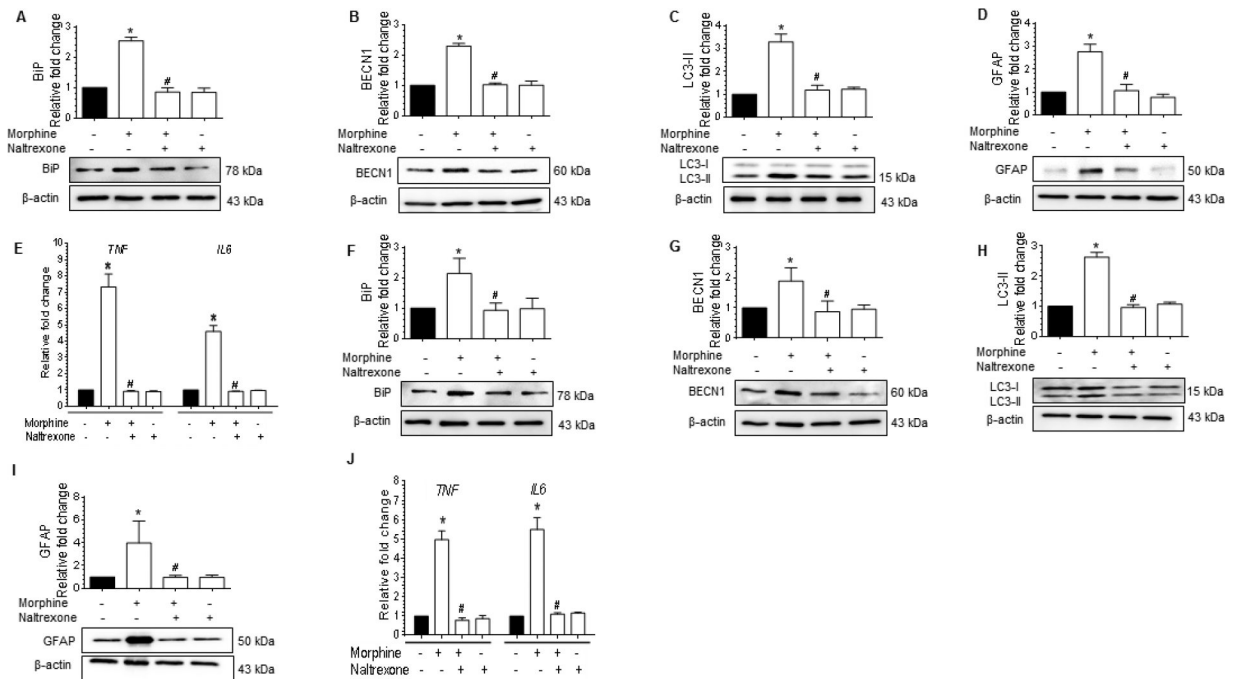


Figure 6. Morphine-mediated defective autophagy involves MOR in astrocytes. (A-D) Representative western blots showing the protein levels of BiP (A), BECN1 (B), LC3-II (C), and GFAP (D) in human A172 astrocytoma cell line pretreated with 100 μ M naltrexone for 1 h followed by 500 nM morphine exposure for 24 h. (E) qPCR showing the relative expression of proinflammatory cytokines such as *TNF* and *IL6* mRNA in human A172 astrocytoma cell line pretreated with 100 μ M naltrexone for 1 h followed by 500 nM morphine exposure for 24 h. (F-J) Representative western blots showing the protein levels of BiP (F), BECN1 (G), LC3-II (H), and GFAP (I) in human primary astrocytes pretreated with 100 μ M naltrexone for 1 h followed by 500 nM morphine for 12 h. (J) qPCR showing the relative expression of proinflammatory cytokines such as *TNF* and *IL6* mRNA in human primary astrocytes pretreated with 100 μ M naltrexone for 1 h followed by 500 nM morphine for 12 h. β -actin was used as a loading control for western blot and *GAPDH* for mRNA expression of cytokines. Data are presented as mean \pm SEM; n = 4. Non-parametric Kruskal-Wallis One-way ANOVA followed by Dunn's *post hoc* test was used to determine the statistical significance between multiple groups: *, P<0.05 vs. control; #, P<0.05 vs. morphine.

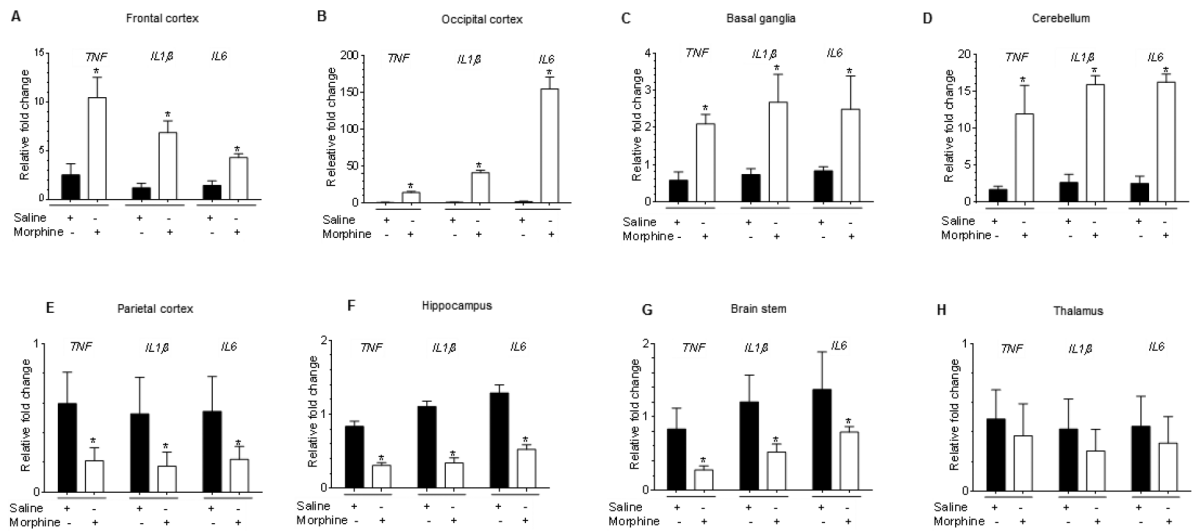


Figure 7. Morphine-dependent rhesus macaques exert brain region-specific upregulation of proinflammatory cytokines. (A-H) qPCR demonstrating the relative expression of proinflammatory cytokines such as *TNF*, *IL1β*, and *IL6* in frontal cortex (A), occipital cortex (B), basal ganglia (C), cerebellum (D), parietal cortex (E), hippocampus (F), brain stem (G), and thalamus (H) of morphine-dependent rhesus macaques. *GAPDH* was used as a loading control for mRNA expression of cytokines. Data are presented as mean ± SEM; n = 4. Abbreviations: S: Saline administered macaques, M: Morphine administered macaques, GCL: Granular cell layer, WM: White matter. Student t test was used to determine the statistical significance: *, P<0.05 vs. saline.

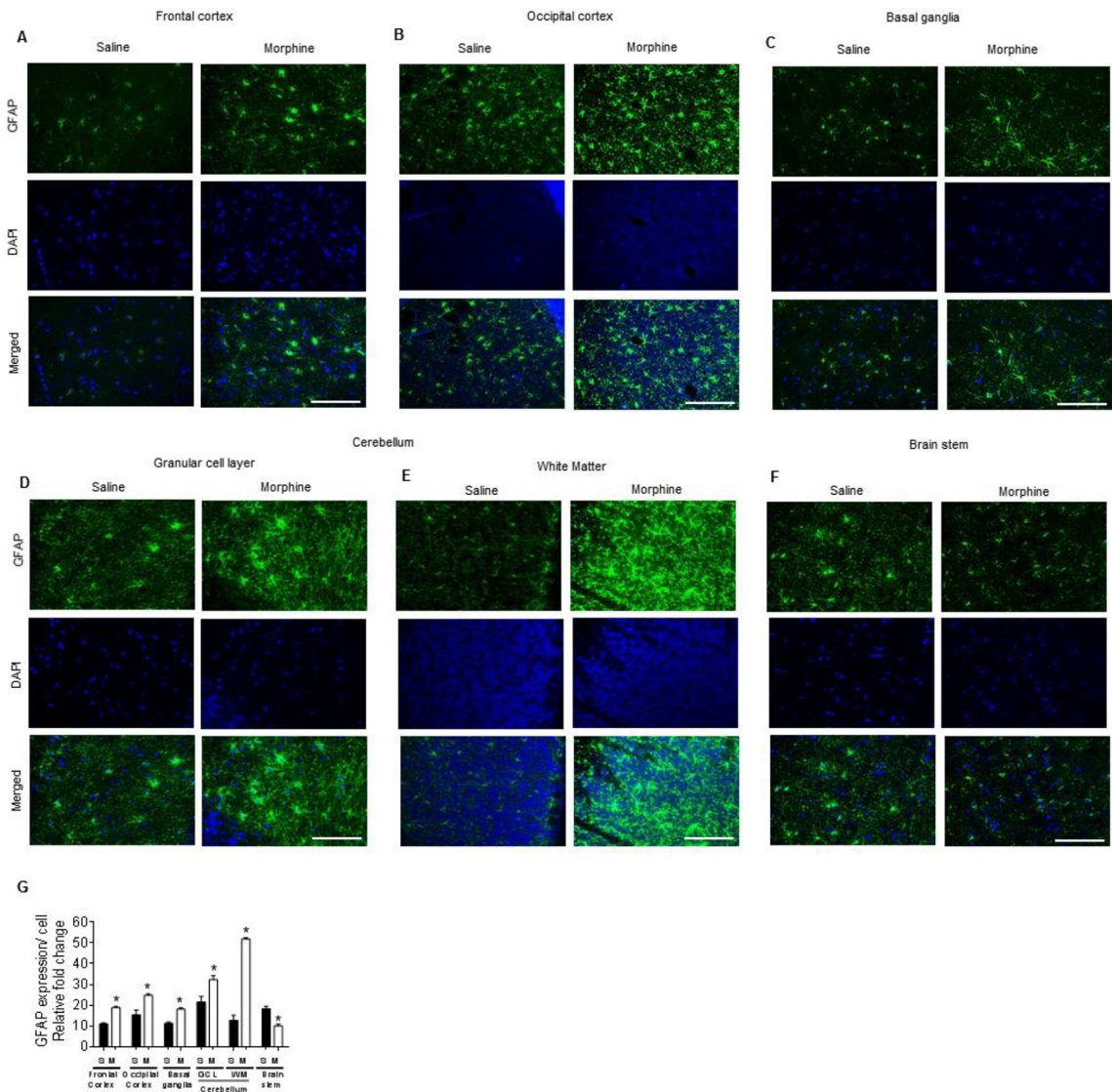


Figure 8. Morphine-dependent rhesus macaques exert brain region-specific activation of astrocytes. A-F) Representative immunohistochemistry images showing the expression of GFAP in frontal cortex (A), occipital cortex (B), basal ganglia (C), different layers of cerebellum – granular layer (D) and white matter (E), and brain stem (F) of morphine-dependent rhesus macaques. Scale bar: 50 μ M. (G) Densitometric analysis of GFAP positive cells using ImageJ software in the frontal cortex, occipital cortex, basal ganglia, different layers of cerebellum—granular layer and white matter, and brainstem of morphine-dependent rhesus macaques. Data are presented as mean \pm SEM; n = 4. Student t test was used to determine the statistical significance: *, P<0.05 vs. saline.

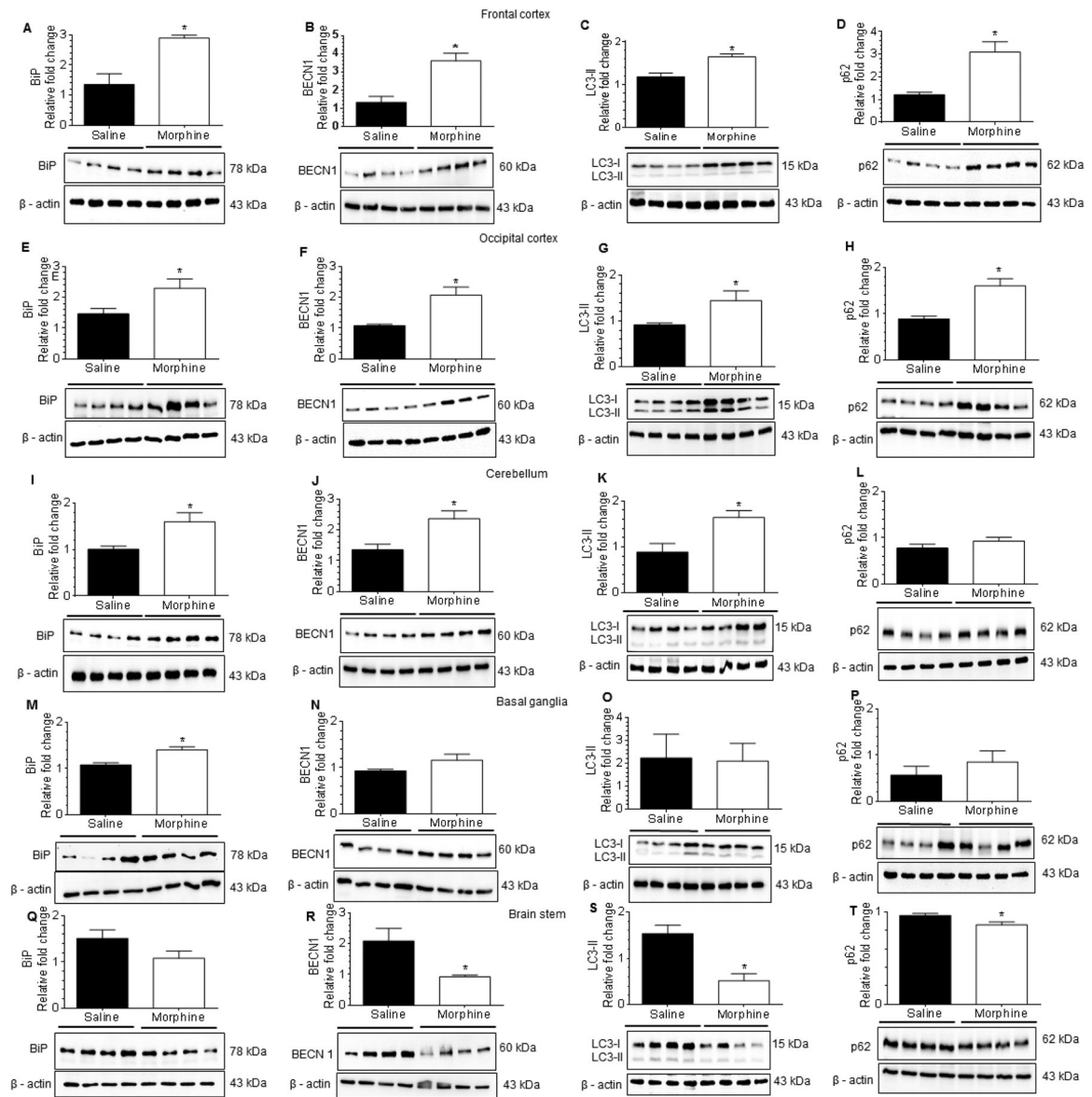


Figure 9. Morphine-dependent rhesus macaques exert brain region-specific activation of astrocytes through ER stress with defective autophagy. (A-D) Representative western blots showing the protein levels of BiP (A), BECN1 (B), LC3-II (C) and p62 (D) in the frontal cortex of morphine-dependent and saline administered rhesus macaques. (E-H) Representative western blots showing the protein levels of BiP (E), BECN1 (F), LC3-II (G) and p62 (H) in the occipital cortex of morphine-dependent and saline administered rhesus macaques. (I-L) Representative western blots showing protein levels of BiP (I), BECN1 (J), LC3-II (K) and p62 (L) in the cerebellum of morphine-dependent and saline administered rhesus macaques. (M-P) Representative western blots showing the protein levels of BiP (M), BECN1 (N), LC3-II (O) and p62 (P) in the basal ganglia of morphine-dependent and saline administered rhesus macaques. (Q-T) Representative western blots showing the protein levels of BiP (Q), BECN1 (R), LC3-II (S) and p62 (T) in the brain stem of morphine-dependent and saline

administered rhesus macaques. β -actin was used as a loading control for all experiments. Data are presented as mean \pm SEM; each group (n = 4). Student's t-test was used to determine the statistical significance: *, P<0.05 vs. saline.

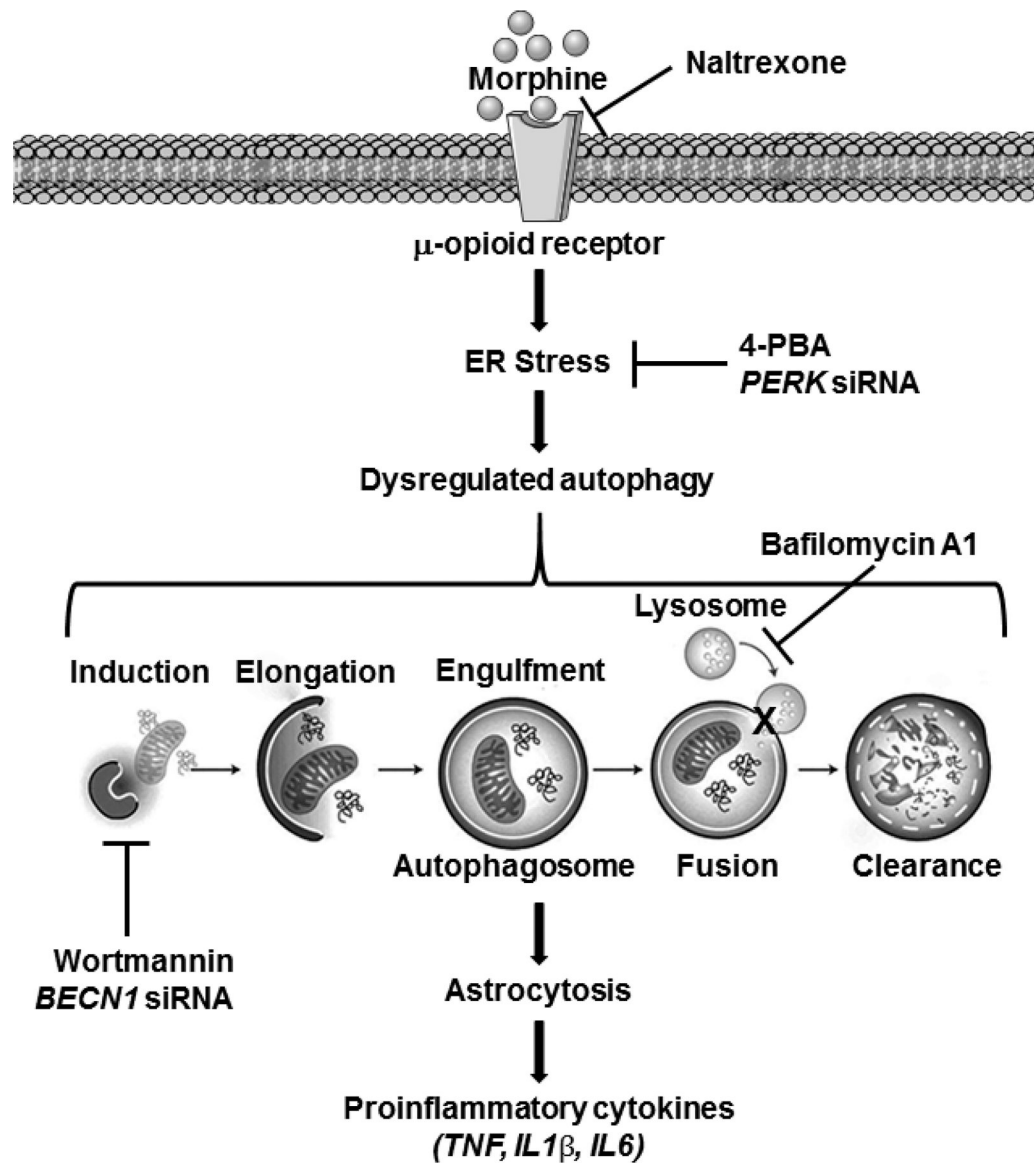


Figure 10.

Schematic diagram showing morphine-mediated activation of astrocytes and secretion of proinflammatory cytokines via MOR-mediated ER stress and defective autophagy. Morphine binds to the MOR in the astrocytes and activates the ER stress. ER stress then induces autophagosome formation but impedes the fusion of autophagosome with the lysosomes leading to defective autophagy. Defective autophagy, in turn, leads to astrocyte activation and proinflammatory cytokines secretion.